Composite octet baryons in a relativistic mean field description of nuclear and neutron star matter

Kaito Noro [1,2,*] Wolfgang Bentz [3,†] Ian C. Cloët [4,‡] and Teruyuki Kitabayashi [3,§]

[1]*Graduate School of Science and Technology, Tokai University, 4-1-1 Kitakaname, Hiratsuka-shi, Kanagawa 259-1292, Japan*
[2]*Micro/Nano Technology Center, Tokai University, 4-1-1 Kitakaname, Hiratsuka-shi, Kanagawa 259-1292, Japan*
[3]*Department of Physics, School of Science, Tokai University, 4-1-1 Kitakaname, Hiratsuka-shi, Kanagawa 259-1292, Japan*
[4]*Physics Division, Argonne National Laboratory, Argonne, Illinois, 60439, USA*

(Received 27 August 2023; revised 18 December 2023; accepted 8 January 2024; published 15 February 2024)

We examine the properties of composite octet baryons in the nuclear medium and neutron-star matter. The internal quark-diquark structure of the octet baryons and the equations of state of nuclear matter and neutron-star matter in the mean field approximation are described by using the three-flavor Nambu–Jona-Lasinio (NJL) model as an effective quark theory of quantum chromodynamics. After introducing our model, we first discuss the properties of single baryons and their effective meson exchange interactions in symmetric nuclear matter by using concepts of Fermi-liquid theory. Several model-independent implications of this description are derived and illustrated by numerical results obtained in our model. Second, we extend the model description to high baryon densities and investigate the equation of state of neutron-star matter and the resulting star masses. We find that the so-called hyperon puzzle persists also for the case of composite hadrons. To get more information on this point, we also investigate the role of 6-Fermi and 8-Fermi interactions, in addition to the standard 4-Fermi interactions. The strengths of those higher-order Fermi interactions is determined so as not to spoil the saturation properties of nuclear matter. Among them, an interaction characterized by a product of four-quark current operators plays a special role to stabilize the stars over a large region of central baryon densities, although it has little effect on the maximum star masses.

DOI: 10.1103/PhysRevC.109.025205

I. INTRODUCTION

Systems of strongly interacting baryons are fascinating objects of current research, because their properties reflect the basic interaction between baryons which is intimately related to their quark substructure, and they connect microscopic nuclear systems to macroscopic astrophysical objects such as supernovae and neutron stars. Besides the familiar building blocks of nuclear systems—protons and neutrons made of up (u) and down (d) quarks—baryons, which carry strangeness, are receiving much attention now because experimental and theoretical tools have become available to study their interactions and their role in nuclear and neutron-star matter.

On the theoretical side, the baryon-baryon interactions have been extensively studied by using the meson exchange picture [1,2], effective field theories [3,4], and quantum Monte Carlo calculations [5]. The parameters characterizing the two-body and possible three-body interactions are usually adjusted to scattering data, quark model predictions, or experimental data on nuclei and hypernuclei. Another line of approach, based on nonrelativistic constituent quark models, has been pursued vigorously [6–8], mainly to understand the origin of the short-range repulsion on the basis of the Pauli principle on the quark level [9]. More recent investigations are based on first principles derived from quantum chromodynamics (QCD) [10,11]. These approaches, together, provide vital information to understand the properties of baryonic systems, in particular hypernuclei [12–15], and are useful tools to analyze new data on hyperon-nucleon scattering [16,17].

A test stone for theoretical models was provided by the observation of heavy neutron stars with about two solar masses [18–21]. Because the presence of hyperons usually leads to a softening of the equation of state of neutron-star matter [22], many models were and are still unable to reproduce such heavy stars, and this problem is commonly called the "hyperon puzzle" [23]. For extensive reviews on this subject and possible solutions, see for example Refs. [24,25]. Most of the proposed solutions require additional repulsion between the baryons in the system, either via the exchange of vector mesons with particular forms of their couplings to baryons [26,27], pomeron exchange [28], or new kinds of three-body interactions [29–32]. Another possible solution [33] is based on the idea of a phase transition from nuclear matter to color superconducting quark matter [34,35] at densities below or near the hyperon threshold.

As we mentioned at the beginning of this section, the properties of baryons and their interactions reflect their quark substructure, which changes in the nuclear medium. To study this aspect of the problem over a wide range of densities, relativistic quark models based on QCD are very useful tools.

*Corresponding author: 1ctad005@mail.u-tokai.ac.jp
†bentz@keyaki.cc.u-tokai.ac.jp
‡icloet@anl.gov
§teruyuki@keyaki.cc.u-tokai.ac.jp

Two models of this kind, which have been used to describe nuclear phenomena in terms of quark degrees of freedom, are the quark-meson-coupling (QMC) model [36], which is based on the MIT bag model [37] and the Nambu–Jona-Lasinio (NJL) model [38–41], for which a full Faddeev approach [42] and a closely related but much simpler quark-diquark approach [43] to baryons have been developed. The degrees of freedom in the QMC model are quarks coupled to elementary mesons via Yukawa couplings, while the NJL model in its original form uses 4-Fermi interactions between quarks to generate mesons as quark-antiquark bound states. Both models have been used extensively to explore the effects of medium modification on the quark level to nuclear observables [44–49].

The QMC model has also been applied to a wide range of hypernuclei [50]. Because meson exchange interactions usually tend to overbind the Λ and Σ baryons in nuclei [4,51], in these earlier calculations a phenomenological repulsive interaction was introduced in order to reproduce the data. In a later version [52], the observation was made that the effect of spin-spin correlations between quarks, associated with the hyperfine interaction from gluon exchange, become enhanced in the nuclear medium if the u and d quark masses decrease as functions of the density but the strange (s) quark mass remains constant. (For a simplified argument, see also Ref. [53].) Because of the different spin-flavor structures of the Λ and Σ baryons, this leads to the expectation that the $\Sigma - \Lambda$ mass difference increases with the nuclear density. This kind of mechanism relies on the assumption of a constant s quark mass, which is well satisfied in hypernuclei where the density of s quarks is essentially zero, but may become less effective in neutron-star matter as soon as a finite density of strange baryons appears.

In the present work, we use the NJL model to describe the internal quark-diquark structure of the octet baryons, the equation of state of nuclear and neutron-star matter in the mean field approximation, the corresponding in-medium effective meson exchange interactions between the baryons, and the resulting neutron-star masses. The purposes of our work are as follows: First, we wish to explore the role of the quark-diquark substructure of baryons in the nuclear medium. For this purpose, we extend our previous work [54] on the properties of octet baryons in free space. Our model is well suited to examine the above expectation about the in-medium $\Sigma - \Lambda$ mass difference, because the spin-spin correlations in the scalar (0^+) and axial vector (1^+) diquark channels are built in from the outset. Second, in close connection to this, we wish to introduce ideas of the successful theory of Fermi liquids due to Landau [55–57] and Migdal [58,59], and its relativistic extensions [60] to hyperons in the nuclear medium. Because the power of the Fermi-liquid theory to respect symmetries, conservation laws, and the renormalization group in many-fermion systems is well known [61–63], we find it desirable and timely to provide such a connection. Third, we wish to present a consistent formulation of isospin-asymmetric baryonic systems on the background of the three independent Lorentz scalar and Lorentz vector mean fields, which are defined in Eq. (2) of the following section. Finally, we wish to investigate the status of the hyperon puzzle in the NJL model and investigate the roles of 6-Fermi [64] and 8-Fermi [65] interactions on the equation of state and star masses in the mean field approximation. To achieve these aims as clearly as possible, we make no attempt to reproduce any empirical data related to octet baryons, their mutual interactions, or properties of neutron stars. Rather than this, we wish to explain problems which arise from chiral symmetry restrictions on the form of the interaction Lagrangian, which were not encountered in our previous work on the flavor SU(2) case [66].

The outline of the paper is as follows: Section II discusses our effective quark model for octet baryons and baryonic matter. Section III discusses the properties of baryons and their effective meson exchange interactions in symmetric nuclear matter using concepts of Fermi liquid theory. Section IV presents our results for neutron-star matter and the resulting star masses. Section V discusses the roles of 6-Fermi and 8-Fermi interactions, and Sec. VI gives a summary of our results.

II. MODEL FOR BARYONS AND BARYONIC MATTER

The three-flavor NJL Lagrangian with 4-Fermi interactions in the $\bar{q}q$ channels relevant for this study reads [40,41]

$$\begin{aligned}\mathcal{L} = {} & \bar{q}(i\partial\!\!\!/ - \hat{m})q + G_\pi[(\bar{q}\lambda_a q)^2 - (\bar{q}\lambda_a\gamma_5 q)^2] \\ & - G_v[(\bar{q}\lambda_a\gamma^\mu q)^2 + (\bar{q}\lambda_a\gamma^\mu\gamma_5 q)^2],\end{aligned} \tag{1}$$

where $q = (q_1, q_2, q_3)$ with $1 \equiv u$, $2 \equiv d$, $3 \equiv s$ being the quark field and $\hat{m}$ the current quark mass matrix with diagonal elements (m_u, m_d, m_s), and λ_a ($a = 0, 1, 2, \ldots 8$) are the Gell-Mann flavor matrices plus $\lambda_0 = \sqrt{2/3}\mathbf{1}$. The 4-Fermi coupling constants in the scalar–pseudoscalar and the vector–axial vector channels are denoted by G_π and G_v, respectively. The Lagrangian (1) has the $\mathrm{SU}(3)_L \otimes \mathrm{SU}(3)_R \otimes \mathrm{U}(1)_V \otimes \mathrm{U}(1)_A$ symmetry of QCD, which contains the familiar flavor SU(3) as a subgroup. The explicit breaking of the $\mathrm{U}(1)_A$ symmetry, which is known as the axial anomaly in QCD, can be realized in the NJL model by the 6-Fermi (determinant) interaction [64], which will be investigated together with possible 8-Fermi interactions in Sec. V. It is important to note that in this work we follow the successful path established by various low-energy theorems and octet mass formulas, that current quark masses are the only sources of explicit breaking of the flavor and the chiral symmetries, and all other symmetry breakings are dynamical. As we will see, this leads to very strong, sometimes unwelcome, restrictions on the model parameters in the mean field approximation.

To construct the octet baryons as quark-diquark bound states, we also need the interaction Lagrangian in the qq channels with the same symmetries, which is specified in Appendix A. Our model description of the octet baryons is a straightforward extension of the quark-diquark model based on the Faddeev framework, as described in Refs. [54,67], to the case where the isospin symmetry is broken, like in neutron-star matter. In the vacuum isospin symmetry is assumed to be intact, i.e., we use $m_u = m_d \equiv m$ throughout this work.

A. Mean field approximation

To construct the equation of state of nuclear matter and neutron-star matter in the mean field approximation, we take into account three scalar fields σ_α and three 4-vector fields ω_α^μ, where $\alpha = u, d, s$. We use the following definitions:

$$\sigma_\alpha = 4G_\pi \langle \bar{q}_\alpha q_\alpha \rangle, \quad \omega_\alpha^\mu = 4G_v \langle \bar{q}_\alpha \gamma^\mu q_\alpha \rangle, \tag{2}$$

where $\langle \dots \rangle$ denotes the expectation value in the ground state of the medium under consideration (vacuum, nuclear matter, or neutron-star matter). The presence of the scalar fields leads to spontaneous breaking of the chiral symmetry and gives rise to the effective quark masses

$$M_\alpha = m_\alpha - \sigma_\alpha, \tag{3}$$

which must be treated independently if the isospin symmetry is broken in the medium. The presence of the vector fields leads to shifts in the four-momenta of the particles in the system. As a result, the energy of a baryon with flavor b and three-momentum $\boldsymbol{k}$ is obtained from the pole of the quark-diquark equation in the variable k_0 as[1]

$$\varepsilon_b(k) = \sqrt{\boldsymbol{k}_b^2 + M_b^2} + n_{\alpha/b}\omega_\alpha^0 \equiv E_b(k_b) + n_{\alpha/b}\omega_\alpha^0, \tag{4}$$

where $n_{\alpha/b}$ is the number of quarks with flavor α in the baryon b, and $\boldsymbol{k}_b = \boldsymbol{k} - n_{\alpha/b}\boldsymbol{\omega}_\alpha$. The effective mass of the baryon, M_b, is a function of the effective quark masses M_u, M_d, M_s, as described in Appendix A.

The mean field approximation is implemented into the Lagrangian (1) in the standard way by decomposing the various quark bilinears into classical (c number) parts and quantum (normal ordered) parts. We assume that the only nonvanishing classical parts are the mean fields given in Eq. (2). The normal ordered parts, together with the qq interaction parts given in Appendix A, are used to calculate bound-state masses of pseudoscalar mesons and octet baryons, as well as the pion decay constant.

The quantity of central interest in our work is the energy density $\mathcal{E}$ of baryonic matter in the mean field approximation. The basic physical picture can be visualized by composite baryons moving in scalar and vector mean fields on the background of the constituent quark vacuum [43]. Except for the vacuum contributions, this is similar in spirit to the QMC model [36,68], although the mesons in our approach are composite objects. The term which describes the Fermi motion of the baryons is given by (note our summation convention for multiple flavor indices)

$$2\int \frac{\mathrm{d}^3k}{(2\pi)^3}\varepsilon_b(k)n_b(k) = 2\int \frac{\mathrm{d}^3k}{(2\pi)^3}E_b(k)n_b(k) + \rho_\alpha\omega_\alpha^0 \equiv \mathcal{E}_B + \rho_\alpha\omega_\alpha^0, \tag{5}$$

where $n_b(k)$ is the Fermi distribution function of baryon b, and we defined the quark number densities ρ_α in terms of the baryon number densities ρ_b by $\rho_\alpha = n_{\alpha/b}\rho_b$. For the case of neutron-star matter we also include the contributions from the Fermi gas of leptons ($\ell = e^-, \mu^-$) in chemical equilibrium with the baryons. The total energy density in the mean field approximation is then expressed as

$$\mathcal{E} = \mathcal{E}_{\mathrm{vac}} - \frac{\omega_\alpha^2}{8G_v} + \rho_\alpha\omega_\alpha^0 + \mathcal{E}_B + \mathcal{E}_\ell. \tag{6}$$

Here the unregularized form of the vacuum (Mexican hat shaped) contribution is

$$\mathcal{E}_{\mathrm{vac}} = 6i\int \frac{\mathrm{d}^4k}{(2\pi)^4}\ln\frac{k^2 - M_\alpha^2}{k^2 - M_{\alpha 0}^2} + \frac{\sigma_\alpha^2 - \sigma_{\alpha 0}^2}{8G_\pi}, \tag{7}$$

where a sum over the quark flavors α is implied, and the subindex 0 refers to the vacuum with zero baryon density.

The scalar and vector fields are determined for given baryon density ρ_B by the conditions

$$\partial\mathcal{E}/(\partial\sigma_\alpha) = \partial\mathcal{E}/\big(\partial\omega_\alpha^\mu\big) = 0. \tag{8}$$

For the scalar fields, the minimizations (8) have to be done numerically. It is, however, easy to confirm that they are equivalent to the relation

$$\sigma_\alpha = 4G_\pi\frac{\partial\mathcal{E}}{\partial m_\alpha} = 4G_\pi\frac{\partial\mathcal{E}}{\partial M_\alpha}, \tag{9}$$

where the first equality is the general Feynman-Hellman theorem, while the second equality holds if the energy density is expressed in such a way that the constituent quark masses M_α always appear together with the current quark masses m_α, i.e., in the first term of the vacuum energy (7) and in the term $\mathcal{E}_B$ of (5). For the vector fields, Eq. (8) leads to

$$\omega_\alpha^\mu = 4G_v j_\alpha^\mu = 4G_v n_{\alpha/b} j_b^\mu, \tag{10}$$

where $j_\alpha^\mu = (\rho_\alpha, \boldsymbol{j}_\alpha)$ is the contribution to the baryon current carried by the quark of flavor α, and j_b^μ is the corresponding quantity for the baryon b. Equation (10) is in accordance with the definition given in Eq. (2).

For neutron-star matter, the minimization with respect to the scalar fields—or equivalently the solution to Eq. (9)—has to be done under the requirements of chemical equilibrium and charge neutrality [22]

$$\mu_b - \mu_n + q_b\mu_e = \mu_\mu - \mu_e = q_i\rho_i = 0, \tag{11}$$

where the chemical potentials for baryons and leptons are given by $\mu_b = \varepsilon_b(k = p_b)$ and $\mu_\ell = (p_\ell^2 + m_\ell^2)^{1/2}$. The Fermi momenta p_i of baryons ($i = b$) and leptons ($i = \ell$) are related to their number densities ρ_i by $\rho_i = p_i^3/3\pi^2$. In Eq. (11), q_i are the electric charges of baryons and leptons. In the general case, for given baryon density, the nine independent relations

[1]Here and in the following, a summation over multiple flavor indices ($\alpha, \beta, \dots$ for quarks, b, b' for octet baryons, τ for the special case of nucleons, and i for baryons and leptons) in a product, including squares like ω_α^2, is implied if those indices appear only on one side of an equation. (As usual, the same convention is used for the Lorentz indices $\mu, \nu, \dots$.) The Fermi momentum of particle i will be denoted as p_i.

in Eq. (11) determine the densities of 10 particles in the system (eight baryons and two leptons). The pressure of the system can then be obtained as a function of baryon density from the relation $P = \rho_i\, \mu_i - \mathcal{E}$.

B. Effective baryon-baryon interaction

For the purpose of discussion, it will be useful to know the form of the effective baryon-baryon interaction which underlies the mean field approximation described above. For this purpose, we follow the ideas of the Fermi-liquid theory [58,61] and its relativistic extensions [60], and define the spin averaged effective baryon-baryon interaction $F_{bb'}(p, p')$ by the variation of the energy of one of the baryons, $\varepsilon_b(p)$, with respect to the distribution function of the other baryon, $n_{b'}(p')$. We wish to express this interaction as a generalized meson-exchange potential. Because our baryon energies in Eq. (4) do no depend explicitly on the distribution functions, we have

$$F_{bb'} = \frac{\delta\varepsilon_b}{\delta n_{b'}} = \frac{\partial\varepsilon_b}{\partial\sigma_\alpha}\frac{\delta\sigma_\alpha}{\delta n_{b'}} + \frac{\partial\varepsilon_b}{\partial\omega_\alpha^\mu}\frac{\delta\omega_\alpha^\mu}{\delta n_{b'}}, \tag{12}$$

where we omitted the dependence on the momenta p and p' to simplify the notations. Because the conditions given in Eq. (8) hold for any fixed set of distribution functions, we can make use of the relations

$$\begin{aligned}\frac{\delta}{\delta n_{b'}}\left(\frac{\partial\mathcal{E}}{\partial\sigma_\alpha}\right) = 0 &= \frac{\partial\varepsilon_{b'}}{\partial\sigma_\alpha} + \frac{\partial^2\mathcal{E}}{\partial\sigma_\alpha\partial\sigma_\beta}\frac{\delta\sigma_\beta}{\delta n_{b'}},\\ \frac{\delta}{\delta n_{b'}}\left(\frac{\partial\mathcal{E}}{\partial\omega_\alpha^\mu}\right) = 0 &= \frac{\partial\varepsilon_{b'}}{\partial\omega_\alpha^\mu} + \frac{\partial^2\mathcal{E}}{\partial\omega_\alpha^\mu\partial\omega_\beta^\nu}\frac{\delta\omega_\beta^\nu}{\delta n_{b'}},\end{aligned} \tag{13}$$

where the second equalities hold in our model when the whole system is at rest, in which case there are no mixings between scalar and vector mean fields. Using (13) in (12) we obtain

$$\begin{aligned}F_{bb'} = &-\frac{M_b}{E_b}\frac{\partial M_b}{\partial\sigma_\alpha}(S^{-1})_{\alpha\beta}\frac{\partial M_{b'}}{\partial\sigma_\beta}\frac{M_{b'}}{E_{b'}} - n_{\alpha/b}(V^{-1})^{00}_{\alpha\beta}n_{\beta/b'}\\ &-\frac{p_i}{E_b}n_{\alpha/b}(V^{-1})^{ij}_{\alpha\beta}n_{\beta/b}\frac{p'_j}{E_{b'}}.\end{aligned} \tag{14}$$

Here $E_b \equiv E_b(p)$, $E_{b'} \equiv E_{b'}(p')$, and we defined the 3×3 flavor matrices S and V by

$$S_{\alpha\beta} \equiv \frac{\partial^2\mathcal{E}}{\partial\sigma_\alpha\partial\sigma_\beta}, \quad V^{\mu\nu}_{\alpha\beta} \equiv \frac{\partial^2\mathcal{E}}{\partial\omega_{\alpha\mu}\partial\omega_{\beta\nu}}. \tag{15}$$

We illustrate the effective interaction of Eq. (14) by Fig. 1, where the solid lines express the baryons, the dashed line expresses the generalized propagators of neutral scalar mesons (S^{-1}) and vector mesons (V^{-1}) for zero momenta, and the vertices stand for the factors to the left and the right of the meson propagators in Eq. (14).

In isospin asymmetric baryonic matter, like neutron-star matter, the $\bar{u}u$, $\bar{d}d$, and $\bar{s}s$ components of the exchanged mesons are mixed by the baryon loop term $\mathcal{E}_B$. To disentangle them, one could make an orthogonal transformation to diagonalize S and V at fixed baryon density, and express the couplings of each exchanged flavor to the baryon by a linear combination of vertices. In the present work we will not carry out such an analysis for the case of neutron-star matter. In the case of isospin symmetric nuclear matter, on the other hand, the matrices S and V become diagonal automatically by taking isoscalar and isovector combinations of the interacting baryons in the particle-hole channel (t channel), and we show the explicit forms in the next section.

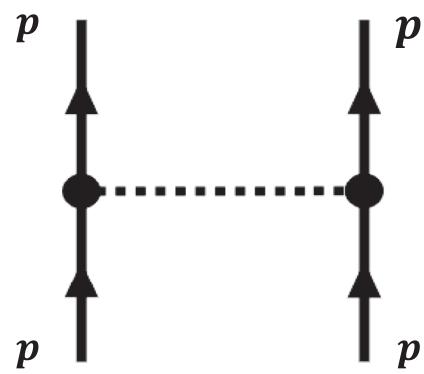

FIG. 1. Graphical representation of the effective baryon-baryon interaction (14) as a meson exchange potential. For explanation of symbols, see the text.

III. BARYONS IN SYMMETRIC NUCLEAR MATTER

In this section we wish to discuss our results for the properties of baryons and their mutual effective meson exchange interactions in isospin-symmetric nuclear matter. In this case, the mean fields (2) with $\alpha = u$ and $\alpha = d$ are the same because of the isospin symmetry, and $\omega_s^\mu = 0$ because the density of strange quarks is zero. Because the s-quark mass enters only in the vacuum energy (7), the minimization condition $\partial\mathcal{E}/\partial\sigma_s = 0$ gives $\sigma_s = \sigma_{s0}$ and therefore $M_s = M_{s0}$. (Note that this holds only in the present case of 4-Fermi interactions. The 6-Fermi and 8-Fermi interactions considered in Sec. V lead to a slight density dependence of M_s even in symmetric nuclear matter.) The energy density of the system is given by Eq. (6) without the leptonic term $\mathcal{E}_\ell$.

A. Effective meson exchange interaction

In the case of isospin-symmetric nuclear matter, the flavor matrices of Eq. (15), which characterize the effective interaction (14), become diagonal automatically by taking appropriate combinations, e.g., for the case of the baryon-nucleon interaction we define

$$f_{bN} \equiv \tfrac{1}{2}(F_{bp} + F_{bn}), \quad f'_{bN} \equiv \tfrac{1}{2}(F_{bp} - F_{bn}). \tag{16}$$

Within the isospin multiplet to which the baryon b belongs, f_{bN} is an isoscalar and the same for all members of the multiplet, while f'_{bN} is an isovector proportional to the isospin three-component of the baryon b. We find the explicit

forms

$$f_{bN}(p,p') = -\frac{M_b}{E_b}\frac{M_N}{E_N}\left(\frac{\partial M_b}{\partial M}\right)\left(\frac{\partial M_N}{\partial M}\right)\left[\frac{1}{2G_\pi} + 2g(M) + \rho_N^{(s)}\frac{\partial^2 M_N}{\partial M^2} + \phi_N\left(\frac{\partial M_N}{\partial M}\right)^2\right]^{-1} + \frac{6\left(1+\frac{y_b}{2}\right)}{1/(2G_v)} - 6\left(1+\frac{y_b}{2}\right)\frac{\boldsymbol{p}\cdot\boldsymbol{p}'}{E_b E_N}\left(\frac{1}{2G_v} + \frac{9\rho_B}{E_N}\right)^{-1}, \tag{17}$$

$$f'_{bN}(p,p') = -\frac{M_b}{E_b}\frac{M_N}{E_N}\left(\frac{\partial M_b}{\partial \Delta M}\right)\left(\frac{\partial M_p}{\partial \Delta M}\right)\left[\frac{1}{2G_\pi} + 2g(M) + \rho_N^{(s)}\frac{\partial^2 M_p}{\partial(\Delta M)^2} + \phi_N\left(\frac{\partial M_p}{\partial \Delta M}\right)^2\right]^{-1} + \frac{2t_b}{1/(2G_v)} - 2t_b\frac{\boldsymbol{p}\cdot\boldsymbol{p}'}{E_b E_N}\left(\frac{1}{2G_v} + \frac{\rho_B}{E_N}\right)^{-1}. \tag{18}$$

Here M is the effective mass of u, d quarks, M_N the nucleon mass in symmetric nuclear matter, and the derivatives with respect to $\Delta M \equiv M_u - M_d$ should be evaluated at $M_u = M_d$. The unregularized form of the function $g(M)$ is

$$g(M) = -12i\int \frac{\mathrm{d}^4k}{(2\pi)^4}\frac{k^2+M^2}{(k^2-M^2)^2}, \tag{19}$$

and the scalar density of the nucleon ($\rho_N^{(s)}$) and the function ϕ_N are defined by

$$\rho_N^{(s)} = 2\int \frac{\mathrm{d}^3k}{(2\pi)^3} n_N(k)\frac{M_N}{E_N(k)}, \tag{20}$$

$$\phi_N = 2\int \frac{\mathrm{d}^3k}{(2\pi)^3} n_N(k)\frac{k^2}{E_N(k)^3}. \tag{21}$$

In Eqs. (17) and (18), $E_b \equiv E_b(p)$, $E_N \equiv E_N(p')$, and we used the relations $n_{u/b} + n_{d/b} = 2(1+\frac{y_b}{2})$ and $n_{u/b} - n_{d/b} = 2t_b$ where y_b and t_b are the hypercharge and the isospin three-component of the baryon b.

The interpretation of (17) for the case $b = N$ in terms of the meson exchange processes of Fig. 1 has been discussed in detail in Ref. [43], and the generalization is almost self evident:[2] The first two lines (third line) in (17) correspond to σ (ω) meson exchange, while the first two lines (third line) in (18) correspond to neutral δ (ρ) meson exchange. The coupling constants of a baryon b to the σ (δ) meson are proportional to the derivative of M_b with respect to M (ΔM), while the couplings to the vector mesons (ω and ρ) are determined by the isoscalar and isovector combination of the quark numbers in the baryon. The function $g(M)$ in the denominators of (17) and (18) is the one quark-loop self-energy of the scalar meson in the vacuum, the terms involving the scalar density are the Fermi averages over effective $\sigma\sigma NN$ ($\delta\delta NN$) contact interactions which are induced by the scalar-isoscalar polarizability $\partial^2 M_N/\partial M^2$ [the scalar-isovector polarizability $\partial^2 M_p/\partial(\Delta M)^2$] of the nucleon [69–71], and the terms proportional to ϕ_N are the Fermi averages over the "Z-graph" contributions, which also appear in hadronic theories [72,73]. In our numerical calculations, discussed in Sec. III C, we find that the numerators of the σ and δ exchange parts in (17) and (18) substantially decrease, while their denominators slightly increase as the baryon density increases. The increase of the denominators is partially related to the fact that the scalar-isoscalar and scalar-isovector polarizabilities of nucleons—both being positive—increase as the baryon density increases. The density dependence of the coupling constants and mesons self-energies in (17) and (18) then suppresses the attractive effects of scalar meson exchanges, and at higher densities the vector meson exchanges become dominant. The terms $\propto \boldsymbol{p}\cdot\boldsymbol{p}'$ correspond to the contributions from the exchange of $\boldsymbol{\omega}$ and neutral $\boldsymbol{\rho}$ mesons, and their self-energies arise only from the Fermi averages over the corresponding Z-graphs. More details will be given in Sec. III C 3 and Appendix B.

B. Physical implications of the interaction

To explain some physical implications of the effective meson exchange interactions f_{bN} and f'_{bN} of Eqs. (17) and (18), we extend a few basic points of Fermi-liquid theory to octet baryons in the nuclear medium. In the following discussions, we use the following notation:[3]

(1) $B = N, \Sigma, \Lambda, \Xi$ stands for the isospin multiplets (including the isospin singlet Λ), while b continues to stand for a member of the baryon octet.
(2) f_{BN} denotes the four independent isoscalar baryon-nucleon interactions defined by Eq. (17) with b a member of B.
(3) f'_{BN} denotes the three independent isovector baryon-nucleon interactions ($B = N, \Sigma, \Xi$) defined by Eq. (18) with b a member of B with the largest value of the isospin three-component t_b (i.e., p, Σ^+, and Ξ^0).

[2]To make the connection to the baryon-meson coupling constants and meson masses, the numerator functions and denominator functions (i.e., those parts which involve $1/2G_\pi$ or $1/2G_v$) must be multiplied by the squares of the relevant quark-meson coupling constants, i.e., by $g_\sigma^{(q)2} = g_\delta^{(q)2}$ for the first two lines of (17) and (18), and by $g_\omega^{(q)2} = g_\rho^{(q)2}$ for the third lines. See Appendix B for details.

[3]Recall that "isovector" ($T = 1$) and "isoscalar" ($T = 0$) refers to the particle-hole channel (t channel) of the interacting baryons, not to the isospin of the two incoming baryons.

We also separate the terms $\propto \boldsymbol{p}\cdot\boldsymbol{p}'$, which involve the transfer of one unit of orbital angular momentum ($\ell = 1$) between the baryons, from the other terms which involve no angular momentum transfer ($\ell = 0$):

$$f_{bN} = f_{0,bN} + \cos\theta f_{1,bN}, \quad f'_{bN} = f'_{0,bN} + \cos\theta f'_{1,bN}, \quad (22)$$

and similarly for f_{BN}, f'_{BN}, F_{bp}, and F_{bn}, where θ is the angle between $\boldsymbol{p}$ and $\boldsymbol{p}'$. The parameters $f_{\ell,NN}$ and $f'_{\ell,NN}$ defined in this way agree with the familiar Landau-Migdal parameters, usually denoted by f_ℓ and f'_ℓ.

1. Nucleon density variations

The $\ell = 0$ baryon-nucleon interactions $f_{0,bN}$ and $f'_{0,bN}$ express the change of the baryon energies, ε_b, caused by variations of the Fermi momenta of the background nucleons. If we denote the corresponding variations of nucleon densities by $\delta\rho_\tau$ ($\tau = p, n$), the change of the distribution functions to first order is given by $\delta n_\tau(k) = \frac{\pi^2}{p_\tau^2}(\delta\rho_\tau)\delta(k - p_\tau)$. Then, according to the general definition given by the first equality in Eq. (12), the energy of a baryon b in nuclear matter changes by an amount

$$\delta\varepsilon_b(k) = 2\int \frac{\mathrm{d}^3p}{(2\pi)^3} F_{b\tau}(k, p)\delta n_\tau(p) = F_{0,b\tau}\delta\rho_\tau. \quad (23)$$

Separating the isoscalar from the isovector contributions then gives the general relations

$$\frac{\partial\varepsilon_b(k)}{\partial\rho_B} = f_{0,bN}(k, p_N), \quad \frac{\partial\varepsilon_b(k)}{\partial\rho_{(3)}} = f'_{0,bN}(k, p_N), \quad (24)$$

where $\rho_{(3)} = \rho_p - \rho_n$, and the limit of isospin-symmetric nuclear matter ($\rho_{(3)} \to 0$) is understood. For the case where b is a nucleon, the parameters $f_{0,NN}$ and $f'_{0,NN}$ for $k = p_N$ are related to the incompressibility K and the symmetry energy a_s as follows:

$$K = 9\rho_B\left(\frac{\pi^2}{2p_N E_N} + f_{0,NN}\right), \quad (25)$$

$$a_s = \frac{\rho_B}{2}\left(\frac{\pi^2}{2p_N E_N} + f'_{0,NN}\right). \quad (26)$$

In our model the baryon energy is given by Eq. (4), and by using Eq. (10) in nuclear matter at rest, we have

$$\varepsilon_b(k) = E_b(k) + 12G_v\rho_B\left(1 + \frac{y_b}{2}\right) + 4G_v\rho_{(3)}t_b. \quad (27)$$

Using this in Eq. (24), we see that in our model the $\ell = 0$ baryon-nucleon interaction reflects the density dependence of the baryon effective masses:

$$f_{0,bN}(k, p_N) = \frac{M_b}{E_b(k)}\frac{\partial M_b}{\partial\rho_B} + 12G_v\left(1 + \frac{y_b}{2}\right), \quad (28)$$

$$f'_{0,bN}(k, p_N) = \frac{M_b}{E_b(k)}\frac{\partial M_b}{\partial\rho_{(3)}} + 4G_v t_b. \quad (29)$$

For the case where b is a nucleon, the two terms in $f_{0,NN}$, when multiplied by $9\rho_B$, give the contributions of σ meson and ω meson exchange to the incompressibility. Similarly, the two terms in $f'_{0,NN}$, when multiplied by $\rho_B/2$, give the contributions of δ meson and ρ meson exchange to the symmetry energy.

2. Lorentz invariance

There are two basic requirements from Lorentz invariance in the present context: First, the distribution function of the nucleons is Lorentz invariant: $n'_\tau(k') = n_\tau(k)$, where we use a prime to denote a system which moves with velocity $\boldsymbol{u}$ relative to the reference system which we assume to be at rest, and $k' = \Lambda_{\boldsymbol{u}}k$, where $\Lambda_{\boldsymbol{u}}$ is the Lorentz matrix. A Lorentz transformation then leads to a variation of the distribution function for fixed momentum according to [60] $\delta n_\tau(k) \equiv n'_\tau(k) - n_\tau(k) = -\varepsilon_\tau(k)\boldsymbol{u}\cdot\hat{\boldsymbol{k}}\delta(k - p_\tau)$ to first order in $\boldsymbol{u}$. Second, the change of the energy of a baryon in symmetric nuclear matter, induced by this density variation,

$$\delta\varepsilon_b(k) = 2\int \frac{\mathrm{d}^3p}{(2\pi)^3} F_{b\tau}(k, p)\delta n_\tau(p) = -\boldsymbol{u}\cdot\hat{\boldsymbol{k}}\frac{2p_N^2\varepsilon_N}{3\pi^2} f_{1,bN}(k, p_N), \quad (30)$$

must be equivalent to a Lorentz transformation applied directly to the baryon energy, $\delta\varepsilon_b(k) \equiv \varepsilon'_b(k) - \varepsilon_b(k) = -\boldsymbol{u}\cdot\boldsymbol{k} + \varepsilon_b(k)\boldsymbol{u}\cdot\boldsymbol{v}_b(k)$ to first order in $\boldsymbol{u}$, where $\boldsymbol{v}_b(k) = \boldsymbol{\nabla}_k\varepsilon_b(k)$ is the velocity of the baryon. This requirement leads to the relation

$$\frac{k}{\varepsilon_b(k)} = v_b(k) + \frac{\varepsilon_N}{\varepsilon_b(k)}\frac{2p_N^2}{3\pi^2} f_{1,bN}(k, p_N). \quad (31)$$

In Eqs. (30) and (31), and in all following relations, $\varepsilon_N \equiv \varepsilon_N(p_N)$ is the Fermi energy of the nucleon in symmetric nuclear matter, while the momentum k is arbitrary. For the case where b is a nucleon, Eq. (31) agrees with the relativistic form of the Landau effective mass relation for variable momentum k [60]. The velocity of the baryon is usually expressed in terms of the Landau effective mass $[M_b^*(k)]$ by $v_b(k) \equiv k/M_b^*(k)$. By taking the limits $k \to 0$ on both sides of Eq. (31), we then obtain a simple relation of the form

$$\frac{1}{\varepsilon_b(0)} = \frac{1}{M_b^*(0)} + \frac{\varepsilon_N}{\varepsilon_b(0)}\rho_B\hat{f}_{1,bN}(0, p_N), \quad (32)$$

where we defined $\hat{f}_{1,bN}(p, p')$ such that the "full" $\ell = 1$ interaction [such as, for example, the last term in Eq. (17)] is expressed in the form $(\boldsymbol{p}\cdot\boldsymbol{p}')\hat{f}_{1,bN}(p, p')$.

It is easy to check that our model satisfies the requirement (31): The energy of a baryon with momentum k and the Fermi energy ε_N of a nucleon in symmetric nuclear matter are obtained from (27) by setting $\rho_{(3)} = 0$:

$$\varepsilon_b(k) = E_b(k) + 12G_v\rho_B\left(1 + \frac{y_b}{2}\right), \quad \varepsilon_N = E_N + 18G_v\rho_B, \quad (33)$$

while $f_{1,bN}$, which corresponds to $\boldsymbol{\omega}$ exchange, is given by the last term in Eq. (17) without the factor $\cos\theta$, see Eq. (22). It is then clear that the general relation (31) is valid in our model.

3. Currents carried by baryons

The Lorentz invariance requirement of Eq. (31) is related to the isoscalar $\ell = 1$ Fermi-liquid parameter $f_{1,bN}$. To give an example where also the isovector part enters, let us consider the currents carried by a baryon b moving with momentum

k in nuclear matter, for the case where no momentum is transferred by the external field to the baryon. From gauge invariance and the integral equations for the vertex functions, the Fermi-liquid theory leads to the following result [74] [see also, for example, Eq. (1.33) of Ref. [61] or Eq. (2.16) of Ref. [58]]:

$$\boldsymbol{j}_b^{(X)}(k) = \boldsymbol{v}_b(k) Q_b^{(X)} + 2p_\tau^2 Q_\tau^{(X)} \int \frac{\mathrm{d}\Omega_p}{(2\pi)^3} \hat{\boldsymbol{p}} F_{b\tau}(k, p), \quad (34)$$

where X characterizes the type of current (e.g., $X = B$ for the baryon current, $X = I$ for the isospin current, and $X = E$ for the electric current), and $Q_b^{(X)}$ are the corresponding bare charges of the baryon b, i.e., $Q_b^{(B)} = 1$, $Q_b^{(I)} = t_b$, and $Q_b^{(E)} = q_b$. The second term in Eq. (34) is the backflow due to the nuclear medium.

The magnitude of the baryon current [case $X = B$ in Eq. (34)] can be expressed in a model-independent way by using the Lorentz invariance relation (31)

$$j_b^{(B)}(k) = \frac{k}{\varepsilon_N} - v_b(k)\left(\frac{\varepsilon_b(k)}{\varepsilon_N} - 1\right). \quad (35)$$

For the case of a nucleon at the Fermi surface, Eq. (35) gives the well-known result $j_N^{(B)}(k = p_N) = p_N/\varepsilon_N$, which reduces to the free current p_N/M_{N0} in the nonrelativistic limit.

For the electric current [case $X = E$ in Eq. (34)] we obtain generally

$$j_b^{(E)}(k) = v_b(k) q_b + \frac{1}{2}\left(\frac{k}{\varepsilon_N} - \frac{\varepsilon_b(k)}{\varepsilon_N} v_b(k)\right) + \frac{p_N^2}{3\pi^2} f'_{1,bN}(k, p_N). \quad (36)$$

Here we can insert our model result for $f'_{1,bN}$, given by the last term in Eq. (18) without the factor $\cos\theta$ [see (22)]. We can express the result in terms of an effective angular momentum g factor of the baryon ($g_{\ell,b}$), which we define here—in a naive way—so that it becomes unity for a free proton, i.e., $j_b^{(E)}(k \to 0) \equiv \frac{k}{M_{N0}} g_{\ell,b}$. This gives

$$g_{\ell,b} = \frac{M_{N0}}{M_b}\left[q_b - \frac{3x}{1+9x}\left(1 + \frac{y_b}{2}\right) - \frac{x}{1+x} t_b\right], \quad (37)$$

where $x = 2G_v\rho_B/E_N = \frac{1}{9}(\frac{\varepsilon_N}{E_N} - 1)$ characterizes the strength of the vector interaction. The quantities which depend on the baryon density in (37) are the baryon effective mass M_b and x.

C. Numerical results

To illustrate several physics points of our above discussions, in this section we present numerical results for symmetric nuclear matter.

1. Model parameters

First we explain the choice of our model parameters. The Lagrangian of Eq. (1) contains the coupling constants G_π and G_v, and the current quark masses m and m_s, which are related to the constituent quark masses in the vacuum, M_0 and M_{s0}, by the gap equations (3). The other parameters, which are necessary to define the model, are the infrared (IR) and ultraviolet (UV) cutoffs $\Lambda_{\rm IR}$ and $\Lambda_{\rm UV}$, which are used with the proper-time regularization scheme [75,76], see Appendix C. In this scheme, the UV cutoff is necessary to give finite integrals, while the IR cutoff is necessary to avoid unphysical decay thresholds of hadrons into quarks, thereby simulating one important aspect of confinement. These parameters are determined as follows: The IR cutoff should be similar to $\Lambda_{\rm QCD}$, and we choose $\Lambda_{\rm IR} = 0.24$ GeV. $\Lambda_{\rm UV}$, m, and G_π are determined so as to give a constituent quark mass in vacuum of $M_0 = 0.4$ GeV, the pion decay constant $f_\pi = 0.93$ GeV, and the pion mass $m_\pi = 0.14$ GeV, using the standard methods based on the Bethe-Salpeter equation in the pionic $\bar{q}q$ channel [40,41]. m_s is determined so as to give a constituent s-quark mass in vacuum of $M_{s0} = 0.562$ GeV, which reproduces the observed mass of the Ω baryon $M_\Omega = 1.67$ GeV by using the quark-diquark bound-state equations explained in Appendix A. The vector coupling G_v is determined from the binding energy per nucleon in symmetric nuclear matter ($E_B/A = -16$ MeV) at the saturation density, which becomes $\rho_0 = 0.15$ fm^{-3}. In the present flavor SU(3) NJL model, the vector couplings in the isoscalar and isovector $\bar{q}q$ channels are the same because of constraints from chiral symmetry, and we do not have an independent parameter [like the coupling G_ρ in the flavor SU(2) model used in Ref. [66]] to fit the symmetry energy.[4] The resulting values of the cutoffs, coupling constants in the $\bar{q}q$ channels, and quark masses are shown in Table I. They are identical to those used in Ref. [66] except for the s-quark masses which were not needed there. Two additional model parameters are the coupling constants in the scalar and axial vector qq channels, G_S and G_A of Eq. (A1). As explained in Appendix A, they are fixed to the free nucleon and delta masses ($M_{N0} = 0.94$ GeV, $M_{\Delta 0} = 1.23$ GeV). The resulting free masses of octet baryons are then predictions of the model and are summarized in Table II together with the observed values.

TABLE I. Values for the model parameters which are determined in the vacuum, single hadron, and nuclear matter sectors. The regularization parameters, constituent quark masses in the vacuum (subindex 0) and current quark masses are given in units of GeV, and the coupling constants in units of GeV^{-2}.

$\Lambda_{\rm IR}$	$\Lambda_{\rm UV}$	G_π	G_v	M_0	M_{s0}	m	m_s
0.240	0.645	19.04	6.03	0.40	0.562	0.016	0.273

2. Energies per nucleon and single baryon energies

In the top panel of Fig. 2 we show the binding energies per nucleon ($\mathcal{E}/\rho_B - M_{N0}$) in symmetric nuclear matter (SNM) in comparison to pure neutron matter (PNM). Although we have

[4]Chiral symmetry would allow different vector couplings in the flavor singlet and octet terms of Eq. (1), but in the mean field approximation used here it is easy to check that there remains only one independent vector coupling in any case. This follows from the identity $\sum_{a=0,3,8}(\bar{q}\lambda_a\Gamma q)^2 = 2[(\bar{q}_1\Gamma q_1)^2 + (\bar{q}_2\Gamma q_2)^2 + (\bar{q}_3\Gamma q_3)^2]$ for any Dirac matrix Γ.

TABLE II. Masses of octet baryons (in units of GeV) calculated in the vacuum (subindex 0) by using the coupling constants $G_S = 8.76\ \mathrm{GeV}^{-2}$ and $G_A = 7.36\ \mathrm{GeV}^{-2}$ in the scalar and axial vector diquark channels fitted to the vacuum masses of the nucleon and the Δ baryon, in comparison with the observed values.[a]

	M_{N0}	$M_{\Lambda 0}$	$M_{\Sigma 0}$	$M_{\Xi 0}$
Calc.	0.94	1.12	1.17	1.32
Obs.	0.94	1.12	1.19	1.32

[a]The fact that our calculated masses agree slightly better with the Gell-Mann Okubo octet mass relation [77,78] $M_{N0} + M_{\Xi 0} = \frac{1}{2}(M_{\Sigma 0} + 3M_{\Lambda 0})$ than the experimental values (using either neutral or isospin averaged masses) may be a mere coincidence.

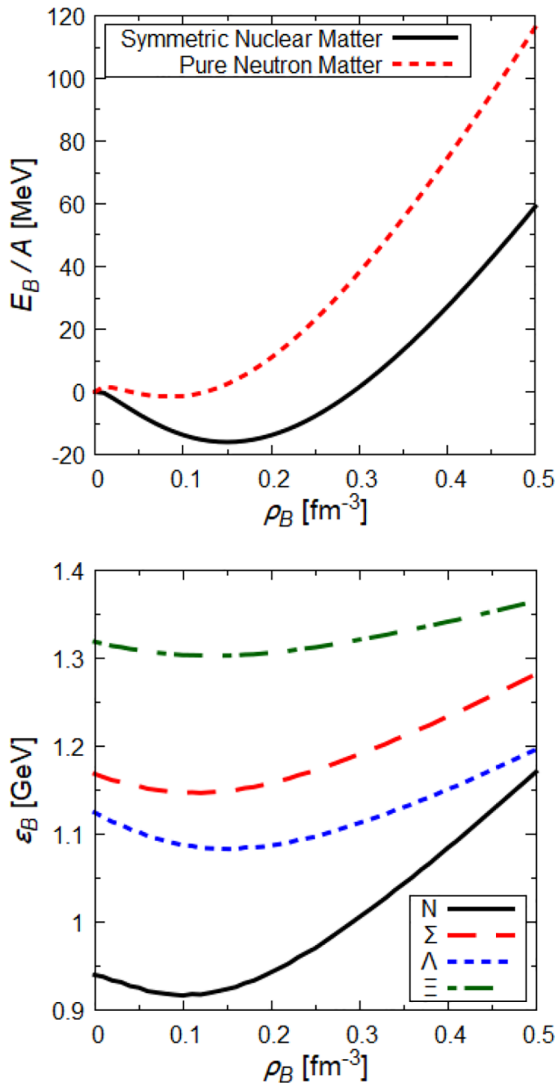

FIG. 2. Binding energy per nucleon in symmetric nuclear matter and pure neutron matter (top panel), and baryon energies ε_B of Eq. (4) in symmetric nuclear matter (bottom panel) as functions of the baryon density. In the bottom panel, the nucleon Fermi momentum is used in ε_N, while the momentum is set to zero for the other baryons.

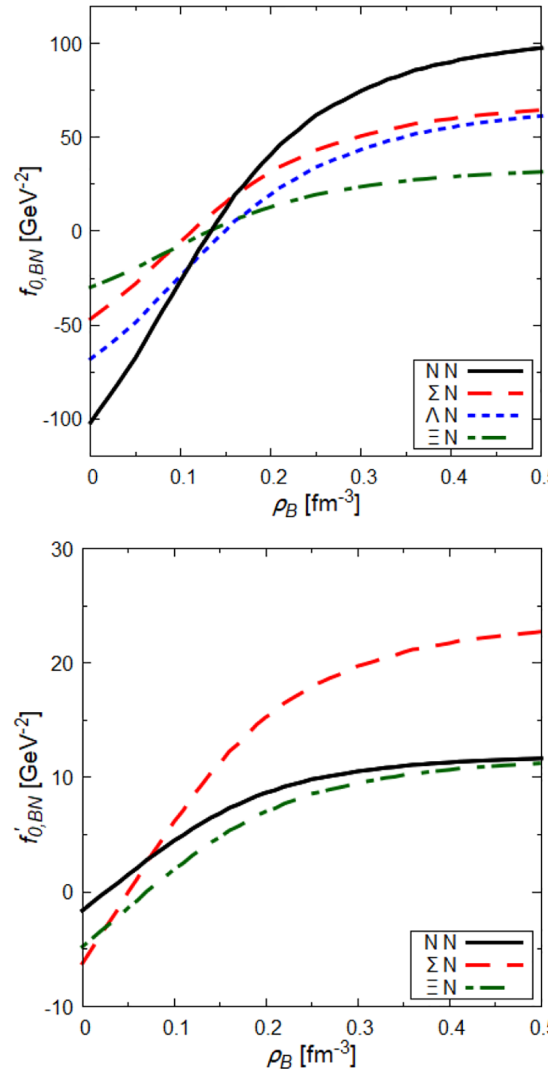

FIG. 3. The $\ell = 0$ part of the isoscalar baryon-nucleon interaction $f_{0,BN}$ (top panel), and the corresponding isovector interaction $f'_{0,BN}$ (bottom panel) in symmetric nuclear matter as functions of the baryon density.

only one parameter G_v to fit the binding energy at saturation in SNM, the result for the saturation density agrees with the empirical value. On the other hand, as we do not have any further free parameters, our results for the incompressibility (symmetry energy) in SNM are too large (too small) compared with the empirical values, as will be discussed in more detail in connection to Fig. 3 later. Because of the small symmetry energy, our PNM is slightly bound around densities of $\rho_B = 0.1\ \mathrm{fm}^{-3}$.

To show the effects of isospin breaking in PNM on the effective quark and nucleon masses, we list in Table III the masses in SNM and PNM for four values of the baryon density. Here we can see several points: First, as can be shown from the gap equation (3), for systems with an excess of d quarks, the magnitude of the mean scalar field σ_d decreases more rapidly with density than the magnitude of σ_u. Therefore $M_u > M_d$, and one can expect that, in an isospin multiplet, the

TABLE III. Effective masses of quarks and nucleons (in units of GeV) in symmetric nuclear matter (SNM) and pure neutron matter (PNM) for four values of the baryon density (in units of fm^{-3}).

Case	ρ_B	M_u	M_d	M_p	M_n
SNM	0	0.4	0.4	0.94	0.94
SNM	0.15	0.325	0.325	0.765	0.756
SNM	0.3	0.284	0.284	0.683	0.683
SNM	0.5	0.257	0.257	0.648	0.648
PNM	0	0.4	0.4	0.94	0.94
PNM	0.15	0.340	0.314	0.768	0.755
PNM	0.3	0.301	0.275	0.695	0.686
PNM	0.5	0.271	0.251	0.656	0.651

baryons with more u quarks will be heavier. Second, as will be explained in detail later, the isospin splittings for the baryons are generally smaller than for the quarks, because of the scalar isovector polarizabilities of the baryons.

In the bottom panel of Fig. 2 we show the Fermi energies (chemical potentials) of the baryons in symmetric nuclear matter. (As the Fermi momenta of hyperons immersed in nuclear matter are zero, the corresponding lines show the energies of hyperons at rest.) The line ε_N shows that nuclear matter is unstable for densities below 0.1 fm^{-3}, and at the saturation density it takes the value $940 - 16 = 924$ MeV. It is seen that the Λ is bound stronger than the nucleon around the saturation density, although its effective mass (not shown here) drops more slowly than M_N with increasing density. The reasons are, first, that the curve for ε_Λ refers to zero momentum, corresponding to low-energy orbitals in finite nuclei, while ε_N refers to the Fermi surface. Second, as shown by Eq. (4), the vector repulsion for the Λ in symmetric nuclear matter ($12G_v\rho_B$) is smaller than for the nucleon ($18G_v\rho_B$) because ω_s^0 vanishes here.

The curves ε_Λ and ε_Σ in Fig. 2 show a quite different behavior. Because in this case the vector repulsion is the same, the increase of the difference between the two lines with increasing baryon density reflects the different dependence of their effective masses on ρ_B. As a result, around the saturation density the Σ is bound by only half of the amount of the Λ, i.e., by about 22 MeV less than the Λ in our model, which is consistent with the estimate of about 20 MeV presented in Ref. [52]. The reason for this lies in the different quark substructure: The scalar diquark made of (u, d) quarks, which is the main source of attraction in the Λ as well as the nucleon, is absent in the Σ as well as in the Δ baryon. This difference in quark structure, which is well known from the constituent quark model [53], generates the mass difference between the free Σ and Λ baryons shown in Table II, and increases with increasing baryon density because the mass of the scalar diquark decreases more rapidly than the mass of the axial vector diquark. The strong (u, d) correlations in the scalar channel, as compared with the axial vector channel, play a role similar to the color magnetic spin-spin interaction from gluon exchange. In our model we adjusted this strength to reproduce the $\Delta - N$ mass difference in free space.

The flattening of the curves ε_B with increasing energy, shown in the lower panel of Fig. 2, continues further to Ξ because in the present model with 4-Fermi interactions the s-quark does not participate in the nuclear interactions in symmetric nuclear matter.

In spite of the increasing $\Sigma - \Lambda$ mass difference due to their different quark substructures, the Σ baryon is still bound in our mean field model. It is now believed that the Σ is unbound in the nuclear medium [13], and recent experiments support this view [17]. It would be natural as a next step to include the effects of antisymmetrization (exchange terms), both on the level of baryons and the level of quarks. It is, in fact, well known that quark exchange effects appear naturally in the hadronization of the NJL model in the path integral formalism [79,80]. The effects of the Pauli exclusion principle on the level of quarks to produce the ΣN repulsion have been emphasized very much recently [9,17]. Since the aim of the present work is to explore the effects of the quark substructure of baryons in a mean field approximation for many baryon systems, we leave this interesting subject for future studies.

3. *Baryon-nucleon Fermi-liquid parameters*

The top panel of Fig. 3 shows the $\ell = 0$ part of the isoscalar baryon-nucleon interaction, given by Eq. (17) without the last term $\propto \boldsymbol{p} \cdot \boldsymbol{p}'$, and the bottom panel shows the corresponding isovector one, Eq. (18). As in the figure for the baryon energies, the momentum of the nucleons is set to the Fermi momentum p_N, and for the hyperons it is set to zero. The behavior of all curves in this figure reflects the change from attraction due to scalar-meson exchange at low densities to repulsion from vector-meson exchange at higher densities. We find that the third and fourth factors in the first lines of (17) and (18), which reflect the couplings of the scalar mesons to the baryons, decrease substantially in magnitude as the density increases, while the denominators given in the second lines of (17) and (18) become slightly enhanced because of cancellations between the attractive quark loop and repulsive baryon loop contributions. Therefore, the attraction from scalar-meson exchange decreases much faster with increasing density than for the case of elementary hadrons. To illustrate this point more quantitatively, we show in Table IV the various factors which characterize the meson-baryon couplings and meson masses in Eqs. (17) and (18). (The full results for the couplings and meson masses, including the effects of the quark-meson couplings, are given in Appendix B.)

The curves in the top panel of Fig. 3 are related to the baryon energies of Fig. 2 by the first of the two general relations given in Eq. (24).[5] It is thus natural that the average values of $f_{0,BN}$ become smaller in the sequence $NN \to \Lambda N \to \Sigma N \to \Xi N$. In particular, as explained above, M_Λ decreases faster with density than M_Σ, and therefore the first term in (28) shows that the ΛN attraction at low densities is stronger than the ΣN attraction. Around the saturation density, the ΛN and the isoscalar ΞN interactions are similar and very small, while

[5]For the case of the nucleon, however, the momentum k is set to the Fermi momentum p_N *after* the differentiation in (24).

TABLE IV. Values of various factors in the effective $\ell = 0$ interactions $f_{0,BN}$ and $f'_{0,BN}$ of Eq. (17) and (18) which characterize the meson-baryon couplings and meson masses, for four values of the baryon density (in units of fm^{-3}). The scalar isoscalar polarizability $(\partial^2 M_N/\partial M^2)$ and the scalar isovector polarizability $[\partial^2 M_p/\partial(\Delta M)^2]$ of the nucleon are given in units of GeV^{-1}, and the denominators D given in the second lines of (17) and (18) are expressed in units of GeV^{-2}.

ρ_B	$\frac{\partial M_N}{\partial M}$	$\frac{\partial M_\Lambda}{\partial M}$	$\frac{\partial M_\Sigma}{\partial M}$	$\frac{\partial M_\Xi}{\partial M}$	$\frac{\partial^2 M_N}{\partial M^2}$	D
0	2.74	1.83	1.55	0.86	5.90	0.0357
0.15	2.07	1.45	1.15	0.65	12.6	0.0398
0.3	1.49	1.14	0.86	0.49	15.9	0.0532
0.5	1.04	0.89	0.63	0.37	17.2	0.0737
ρ_B	$\frac{\partial M_p}{\partial(\Delta M)}$		$\frac{\partial M_{\Sigma^+}}{\partial(\Delta M)}$	$\frac{\partial M_{\Xi^0}}{\partial(\Delta M)}$	$\frac{\partial^2 M_p}{\partial(\Delta M)^2}$	D
0	0.70		1.55	0.86	9.35	0.0357
0.15	0.49		1.15	0.65	14.7	0.0418
0.3	0.33		0.86	0.49	18.1	0.0572
0.5	0.21		0.63	0.37	19.8	0.0819

the isoscalar NN and ΣN interactions are both repulsive.[6] For the NN case, we can use Eqs. (25) and (28) to split the incompressibility as $K = \frac{3p_N^2}{E_N} + 9\rho_B \frac{M_N}{E_N}\frac{\partial M_N}{\partial \rho_B} + 162 G_v \rho_B = (0.253 - 1.014 + 1.124)$ GeV $= 0.363$ GeV, where the first term refers to noninteracting quasiparticles with $E_N = 0.8$ GeV, the second term corresponds to σ meson exchange, and the third term to ω meson exchange. To reproduce the empirical value $K \simeq 0.25$ GeV, we would need $f_{0,NN} \simeq 0$ at saturation density, instead of the positive value indicated in Fig. 3.

The three curves in the lower panel of Fig. 3 similarly result from the attraction due to δ meson exchange at low densities and the repulsion from ρ meson exchange at higher densities. The fact that the isovector ΣN repulsion is stronger than the others is simply because of the isospin factor t_b in Eq. (29), which indicates that the energy of $\Sigma^\pm$ is most sensitive to changes of the isovector nucleon density. The overall size of the isovector interactions is small compared with the isoscalar ones. For the NN case, we can use Eqs. (26) and (29) to split the symmetry energy as $a_s = \frac{p_N^2}{6E_N} + \frac{\rho_B}{2}\frac{M_N}{E_N}\frac{\partial M_p}{\partial \rho_{(3)}} + G_v \rho_B = (14 - 3 + 7)$ MeV $= 18$ MeV, where the first term refers to noninteracting quasiparticles, the second term corresponds to δ meson exchange and the third term to ρ meson exchange. It is known from the case of elementary nucleons [81] that the mechanism of δ meson exchange gives a negative contribution to the symmetry energy, and in our model this effect is small. Our value of a_s is considerably smaller than the empirical value $a_s \simeq 32$ MeV, which reflects the fact that our three-flavor Lagrangian (1) does not allow for an independent vector coupling in the isovector channel because of the assumed flavor and chiral symmetry, in contrast with the two-flavor case [66].

Finally in this section, we add two more comments. The first concerns the isospin splittings which can be expected for isospin asymmetric matter. Because our $f'_{0,BN}$ is negative at small densities, the first term in Eq. (29) is negative for $b = p, \Sigma^+, \Xi^0$. For systems with neutron excess ($\rho_{(3)} < 0$) we can then expect that the in-medium isospin splittings will be ordered such that the particles with more u quarks become heavier, which is consistent with our finding that $M_p > M_n$ and $M_u > M_d$ in neutron rich matter, see Table III. The reason why the mass splittings for baryons are smaller than for quarks is now clear from Table IV, which shows that the isovector couplings $\partial M_b/\partial(\Delta M)$ strongly decrease with increasing baryon density. Expressed in a different way, the scalar isovector polarizability of the nucleon $[\partial^2 M_p/\partial(\Delta M)^2]$ strongly increases with the density.

Second, it is well known that any two-body interaction with nonexplicit density dependence, for example through masses and couplings, contains effects from an effective three-body interaction. Taking the $\ell = 0$ part of Eq. (17) as an example, in the case of point nucleons the only density dependence of this kind resides in the factor M_N/E_N and in the function ϕ_N in the denominator. The decrease of our couplings and the increase of meson masses due to the scalar isoscalar polarizability of the nucleons reflect the presence of additional repulsive three-body interactions.[7] The rapid decrease of the bN attraction with increasing density, expressed by Fig. 3, shows that our effective three-particle interaction is strongly repulsive, but—as Fig. 2 (lower panel) has shown—not sufficient to generate an overall repulsion between the Σ baryon and the nucleon.

4. In-medium orbital g factors of baryons

Here we wish to illustrate the renormalization of the orbital angular momentum g factors, given by Eq. (37), for a few cases. In Sec. III B 3 we used the concept of the backflow, which is central to the Fermi-liquid theory, but the same results can be obtained in relativistic meson-nucleon theories by using the response of the core (filled Fermi sea of nucleons) to the addition of one nucleon [83,84] or one hyperon [85,86]. In such a description, the backflow arises from RPA-type vertex corrections due to virtual $N\overline{N}$ excitations of the core,[8] and the importance of these contributions to give reasonable magnetic

[6] We remind again that $f_{0,BN}$ refers to the spin averaged interaction characterized by $\ell = 0$ and $T = 0$ in the particle-hole channel.

[7] The variation of $f_{0,bN}$ with density can be expressed as an effective three-body interaction:

$$\frac{\delta f_{0,bN}}{\delta \rho_B} = \frac{1}{4}\sum_{\tau=p,n}(h_{0,bp\tau} + h_{0,bn\tau}),$$

where the three-particle forward-scattering amplitudes (h_0) are defined as averages over the angles between the momenta of the three interacting particles [82].

[8] The "antinucleons" which show up in those vertex corrections, or in the Z-graph contributions to the scalar-meson propagators mentioned in Sec. III A, are highly virtual objects, mathematically necessary to form a complete set of spinors, and have little to do with real observable antinucleons.

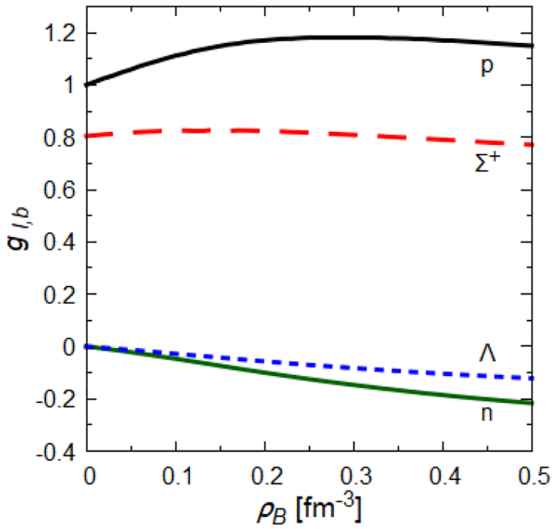

FIG. 4. The angular momentum g factors [see Eq. (37)] of the proton in comparison to the Σ^+, and of the neutron in comparison to the Λ, in symmetric nuclear matter as functions of the baryon density.

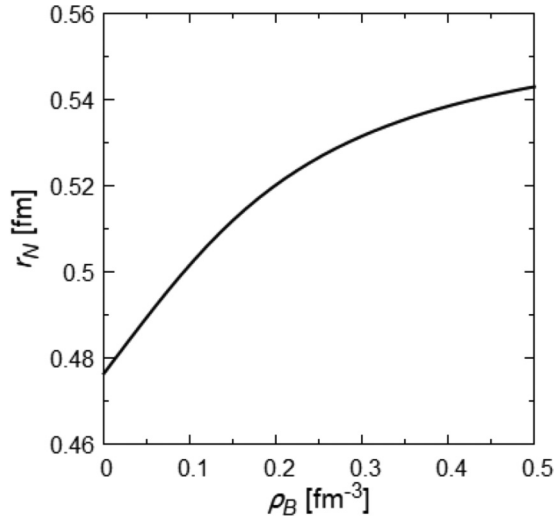

FIG. 5. Rms radius of the baryon density distribution of the quark cores in SNM as function of the baryon density.

moments in relativistic theories is well known [87,88]. As examples for baryons with positive charge, we illustrate the relation (37) for the proton and the Σ^+, and as examples for neutral baryons we show the cases of the neutron and the Λ in Fig. 4. For the isoscalar combination $g_{\ell,p} + g_{\ell,n}$, the backflow reduces the enhancement ($M_{N0}/M_N \simeq 1.24$ near the saturation density) by a factor of $E_N/\varepsilon_N \simeq 0.87$, while for the isovector combination $g_{\ell,p} - g_{\ell,n}$ there is almost no reduction, because the last term in (37) is very small. As a result, the isovector combination remains enhanced, i.e., g_ℓ of the proton (neutron) is larger (smaller) than its free value. For the Σ^+, the enhancement due to its reduced mass is only about half of the case of the proton, and the reduction from the backflow gives results which change only mildly with density. For the Λ, the backflow corrections are similar in magnitude to the case of the neutron, but its effective mass, and therefore also g_ℓ, decreases more slowly with density. For more expensive discussions on backflow effects for the magnetic moments of hypernuclei, we refer to Ref. [86].

5. Comments on sizes of quark cores of in-medium nucleons

Finally, in this section, we wish address the question whether the size of in-medium nucleons invalidates the basic physical picture of the mean field approximation. The relevance of this question is underlined by the fact that the NJL model is known to predict a moderate swelling of nucleons in the medium at normal densities, a feature which is important for the EMC effect [48] or the Coulomb sum rule [49]. If the nucleons swell considerably at higher densities, the Pauli principle would become inapplicable at the nucleon level.

Rather than the physical size of nucleons including their meson clouds, the quantity which seems more relevant for role of the Pauli principle is the size of the quark cores of the nucleons in the medium. Here we consider the rms radius of the baryon density distribution of the quark cores, denoted as $r_N(\rho_B)$, which is an isoscalar quantity and therefore the same for protons and neutrons. The definitions and further details are given in Appendix D, and the results are shown in Fig. 5. Our free nucleon (zero density) value is $r_N(0) = 0.475$ fm, which increases by 7% at saturation density (0.15 fm^{-3}), and by 13% at $\rho_B = 0.5$ fm^{-3}. Even at very large densities ($\rho_B \simeq 1.0$ fm^{-3}) the baryon radius of the quark core increases only by 16% of its free value. This behavior reflects our phenomenological implementation of confinement effects via the infrared cutoff ($\Lambda_{\rm IR}$). It is interesting to note that our values of r_N are similar to the radii which have been assumed in the excluded volume framework in QMC model calculations [89,90], although we do not go into further details here.

By using the values of r_N shown in Fig. 5, we can estimate the volume fractions occupied by the quark cores in SNM (see Appendix D). We obtain 9% at saturation density, and 36% at the highest density shown in the previous figures of this section ($\rho_B = 0.5$ fm^{-3}). Although these numbers may give us some confidence in the overall physical picture of the mean field approximation, they leave room for corrections and improvements of the model. We also recall that the Pauli principle at the quark level has been predicted to play an important role in producing the ΣN repulsion even at normal densities, as mentioned at the end of Sec. III C 2. Further investigations on these points are necessary.

IV. NEUTRON-STAR MATTER

In this section we wish to discuss our results for neutron-star matter and the resulting star masses, based on the expression (6) for the energy density and the equilibrium and charge neutrality conditions (11). Our parameters are the same as used in symmetric nuclear matter, see Sec. III C 1. As mention at the end of Sec. II B, we will not analyze the effective baryon-baryon interactions in neutron-star matter as exhaustively as we have done for nuclear matter in order to keep the length of the paper within reasonable limits.

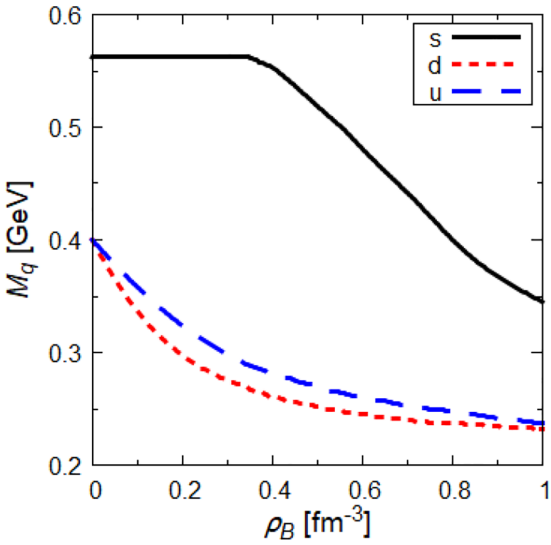

FIG. 6. The effective quark masses in neutron-star matter as functions of the baryon density.

A. Single-particle in-medium properties

First we show our results for the quark effective masses in Fig. 6 as functions of the baryon density. Because of the isospin asymmetry (excess of d quarks) in neutron-star matter, the u quark becomes heavier than the d quark by 25 MeV at baryon densities around 0.3 fm^{-3}. As discussed already in Sec. III C 2, this is expected from $|\sigma_u| > |\sigma_d|$ in neutron-rich matter, or equivalently from the effective δ-meson exchange mechanism [81] in hadronic theories. The s-quark mass, on the other hand, starts to decrease as soon as hyperons appear in the system, i.e., as soon as the condition $\partial\mathcal{E}/\partial\sigma_s = 0$ receives contributions from hyperons in the baryon loop term $\mathcal{E}_B$ of Eq. (6). In this case, the $\bar{s}s$ exchange between hyperons can proceed without violating the OZI rule [91–93], and, as anticipated in Sec. I, this gives rise to an appreciable attraction in neutron-star matter. We explain later how this decrease of M_s influences the masses of neutron stars.

The upper panel of Fig. 7 shows our results for the chemical potentials, and the lower panel shows the density fractions of the particles as functions of the baryon density. The upper panel is the analog of the lower panel of Fig. 2, discussed in the previous section for symmetric nuclear matter. The three solid lines in the upper panel of Fig. 7 (from bottom to top) show $\mu_p = \mu_n - \mu_e$, μ_n, and $\mu_n + \mu_e$. Because of the conditions (11), the density where the chemical potential of a hyperon with electric charge q_b touches the solid line $\mu_n - q_b\mu_e$ from above is the threshold density for this hyperon. Below the threshold densities, the chemical potentials are simply the energies of hyperons at rest (zero Fermi momentum). Compared with the symmetric nuclear matter case of Fig. 2, the lines show a considerable isospin splitting, which mainly comes from the vector potential term in Eq. (4). For example, the vector potential for Σ^- is $4G_v(2\rho_d + \rho_s)$, which is larger than the vector potential for Σ^+, which is $4G_v(2\rho_u + \rho_s)$. The mass splittings are in the opposite order, e.g., Σ^+ is heavier than Σ^-, as can be expected also from

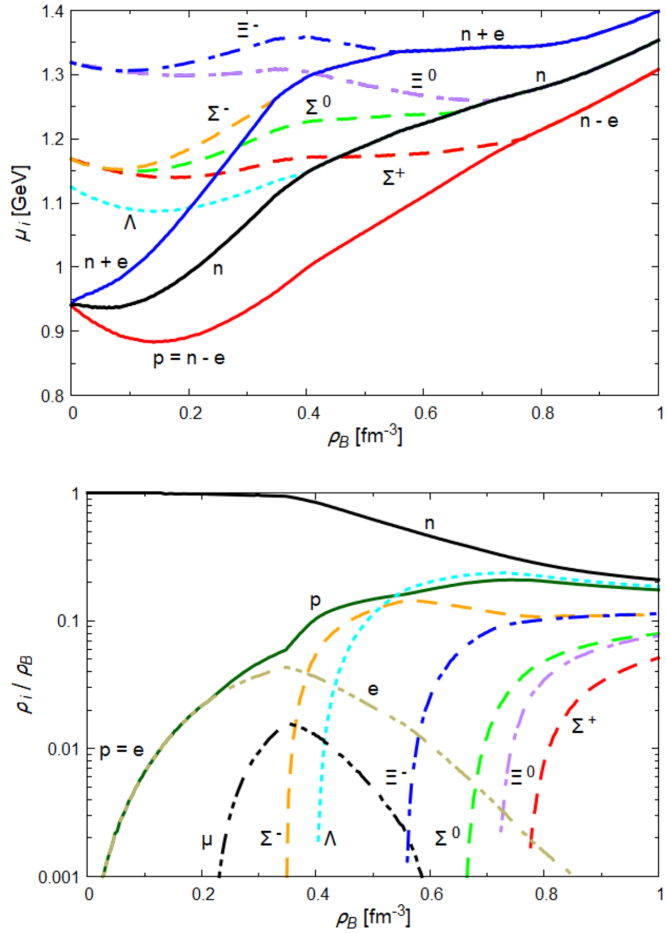

FIG. 7. The chemical potentials of baryons (top panel), and the density fractions of baryons and leptons (bottom panel) in neutron-star matter as functions of the baryon density.

Fig. 6. The mass splittings in baryon isospin multiplets are, however, small compared with the splittings from the vector potential. For example, at baryon densities around 0.3 fm^{-3} the mass splitting between Σ^+ and Σ^- is only about 20 MeV, and the proton-neutron mass difference is only about 10 MeV, both being smaller than the naive expectation from the quark mass difference shown in Fig. 6 for the reasons explained in the previous section. In the low-density region, where $\rho_s = 0$ and $\rho_u + \rho_d = 3\rho_B$, the vector potentials for Σ^0 and Λ are the same $[4G_v(\rho_u + \rho_d)]$, and we see again the different behaviors of their energies with increasing baryon density, which is caused by their different quark substructures, as discussed in Sec. III C 2.

As we can see from Fig. 7, the threshold density for Σ^- is $\rho_B = 0.35$ fm^{-3} in our calculation. Although it has been conjectured for long on energetic reasons that Σ^- will appear as the first hyperon in neutron-star matter [94], this point is controversial nowadays [95–97], mainly because the ΣN interaction is believed to be repulsive (see the related discussions at the end of Sec. III C 2). However, we wish to note that also in our present mean field model the onset of Σ^- depends on several details: First, we are underestimating the free Σ mass by about 20 MeV (see Table II); second, the in-medium

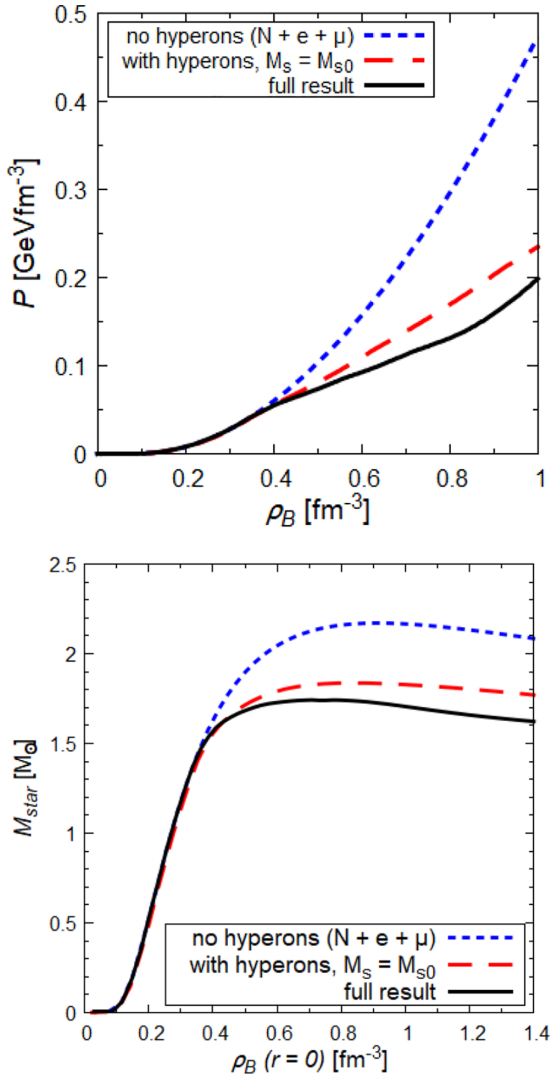

FIG. 8. The pressure in neutron-star matter as function of the baryon density (top panel) and the resulting neutron star masses as functions of the central baryon density (bottom panel). The three lines in each panel show the cases of nucleons and leptons only, the case including hyperons but fixing the s-quark mass to its free value, and the full result obtained with by treating all three quark masses as independent variational parameters.

mass of Σ^- is shifted down by a similar amount relative to Σ^+, as explained above; and third, our electron chemical potential is rather large in this density region. Therefore, apart from the more fundamental problem on the ΣN repulsion, the question whether μ_{Σ^-} touches $\mu_n + \mu_e$ or not, and if it does at which baryon density, depends on several details of the model. (We return to this point in a different context in Sec. VI.)

B. Equation of state and neutron star masses

The upper panel of Fig. 8 shows our results for the pressure in neutron-star matter as function of the baryon density, and the lower panel shows the neutron-star masses, as obtained from the solution of the Tolman-Oppenheimer-Volkoff (TOV) equations [98,99], with the constraints of Eq. (11) imposed, as functions of the central baron density. We show the cases of nucleons and leptons only, the case including hyperons but fixing artificially the effective s-quark mass to its free value M_{s0}, and the full result with the s-quark mass determined by minimization of the energy density. The results for nucleons and leptons only are very similar to the results obtained in Ref. [66] for the flavor SU(2) case, although there it was possible to reproduce the symmetry energy without explicit breaking of chiral symmetry of the interaction Lagrangian. (See Appendix A for a more detailed comparison.)

It is well known that the presence of hyperons can lead to a sizable reduction of the pressure in neutron-star matter and a decrease of the maximum mass of neutron stars [22,23], and Fig. 8 shows that the same situation is encountered in a relativistic mean field calculation which takes into account the internal quark-diquark structure of the octet baryons. Our results suggest that most of the reduction of the pressure arises simply because nucleons and leptons with high Fermi momenta can be converted to hyperons with low Fermi momenta by weak processes. The reduction of the s-quark mass in the medium is not so important for the overall size of the pressure and the maximum star mass, but it works towards destabilization of the star as the central baryon density increases. The values of the maximum central baryon densities which gives stable stars, the maximum star masses, and the radii of the stars with maximum mass for the three cases shown in Fig. 8 are as follows:

$$\left[\rho_{\rm B}^{\rm max}(r=0),\ M_{\rm star}^{\rm max},\ R\right] = (0.9{\rm fm}^{-3},\ 2.17M_\odot,\ 11.5{\rm km})$$

for the case of no hyperons,

$$\left[\rho_{\rm B}^{\rm max}(r=0),\ M_{\rm star}^{\rm max},\ R\right] = (0.85\ {\rm fm}^{-3},\ 1.83M_\odot,\ 11.8\,{\rm km})$$

for the case with hyperons but M_s fixed to M_{s0}, and

$$\left[\rho_{\rm B}^{\rm max}(r=0),\ M_{\rm star}^{\rm max},\ R\right] = (0.72\,{\rm fm}^{-3},\ 1.73\,M_\odot,\ 12.3\ {\rm km})$$

for the case with hyperons and M_s determined from minimization of the energy density.

V. ROLE OF 6-FERMI AND 8-FERMI INTERACTIONS

Because the maximum mass of neutron stars is sensitive to the high-density behavior of the equation of state, it is natural to investigate the role of higher-order Fermi interactions, i.e., the 6-Fermi [64] and 8-Fermi [65] interactions. While there is little doubt about the importance of the 6-Fermi (flavor determinant) interaction to break the $U_A(1)$ symmetry of the 4-Fermi Lagrangian of Eq. (1) and to split the masses of the otherwise degenerate pseudoscalar mesons π and η, the situation is not so clear for the 8-Fermi interactions, because many possible flavor structures are allowed by chiral symmetry. In this work we limit ourselves to three types of chiral-invariant 8-Fermi interactions with the simplest structure, namely, the square of the scalar-pseudoscalar term in Eq. (1), the product of this term with the vector-axial vector term, and the square of the vector-axial vector term. We wish to investigate whether those higher-order Fermi interactions in the $\bar{q}q$ channels, with coupling constants restricted by the basic properties of symmetric nuclear matter around the saturation point, can lead to appreciable changes in high density neutron-star matter or not.

We will not include higher-order interactions in the qq channels used to construct the baryons as quark-diquark bound states, i.e., the Lagrangian of Eq. (A1) is left unchanged.

A. Basic formulas and new parameters

To the basic NJL Lagrangian of Eq. (1), we add the 6-Fermi (flavor determinant) interaction [34]

$$\mathcal{L}_6 = G_6 \det[\bar{q}_\alpha(1-\gamma_5)q_\beta + \bar{q}_\alpha(1+\gamma_5)q_\beta], \tag{38}$$

and the following 8-Fermi interactions:

$$\begin{aligned}\mathcal{L}_8 &= G_8^{(ss)}(\mathcal{L}_s\mathcal{L}_s) - G_8^{(sv)}(\mathcal{L}_s\mathcal{L}_v) - G_8^{(vv)}(\mathcal{L}_v\mathcal{L}_v)\\ &\equiv \mathcal{L}_8^{(ss)} + \mathcal{L}_8^{(sv)} + \mathcal{L}_8^{(vv)}.\end{aligned} \tag{39}$$

Here $\mathcal{L}_s$ means the 4-Fermi interaction in the scalar-pseudoscalar channel of Eq. (1) without the factor G_π, and $\mathcal{L}_v$ means the one in the vector-axial vector channel of Eq. (1) without the factor $(-G_v)$. In this simplest possible form, each factor $\mathcal{L}_s$ or $\mathcal{L}_v$ is closed under the summations over Dirac, flavor, and color indices. Altogether four new coupling constants are involved in (38) and (39).

The mean field approximation is implemented in the same way as for the 4-Fermi interactions in Sec. II A. The gap equation (3) is now replaced by the more complicated form

$$M_\alpha = m_\alpha - \sigma_\alpha\left(1 + \frac{G_8^{(ss)}}{4G_\pi^3}\sigma_\beta^2 - \frac{G_8^{(sv)}}{8G_\pi G_v^2}\omega_\beta^2\right) + \frac{G_6}{8G_\pi^2}\sigma_\beta\sigma_\gamma, \tag{40}$$

where in the 6-Fermi term (α, β, γ) is any set of three different quark flavors, and in the other terms a sum over the quark flavors β is implied. The baryon energies (4) are replaced by

$$\varepsilon_b(k) = E_b(k_b) + n_{\alpha/b}V_\alpha^0, \tag{41}$$

where $\boldsymbol{k}_b = \boldsymbol{k} - n_{\alpha/b}\boldsymbol{V}_\alpha$, with the vector fields V_α^μ defined by

$$V_\alpha^\mu = \omega_\alpha^\mu\left(1 + \frac{G_8^{(sv)}}{8G_\pi^2 G_v}\sigma_\beta^2 + \frac{G_8^{(vv)}}{4G_v^3}\omega_\beta^2\right). \tag{42}$$

The new contributions from the 6-Fermi and 8-Fermi interactions to the energy density are

$$\mathcal{E}_6 = -\frac{G_6}{16G_\pi^3}(\sigma_u\sigma_d\sigma_s - \sigma_{u0}\sigma_{d0}\sigma_{s0}), \tag{43}$$

$$\begin{aligned}\mathcal{E}_8 = {}& \frac{3G_8^{(ss)}}{64G_\pi^4}\left(\sigma_\alpha^2\sigma_\beta^2 - \sigma_{\alpha0}^2\sigma_{\beta0}^2\right) - \frac{3G_8^{(sv)}}{64G_\pi^2G_v^2}\sigma_\alpha^2\omega_\beta^2\\ &- \frac{3G_8^{(vv)}}{64G_v^4}\omega_\alpha^2\omega_\beta^2,\end{aligned} \tag{44}$$

which are added to Eq. (6), after replacing ω_α^μ in (6) by the expression given in Eq. (42). It is easy to check that the basic conditions (8), which determine the three scalar and three vector mean fields σ_α and ω_α^μ, lead to the same expressions (9) and (10) as before, because those expressions simply reflect the definitions given by Eq. (2). If we eliminate the vector fields by using (10), it becomes clear that $G_8^{(ss)}$ and $G_8^{(vv)}$ must be positive in order that the energy density is bounded from below, while the sign of $G_8^{(sv)}$ is not determined generally. For the case of neutron-star matter, the conditions of chemical equilibrium and charge neutrality are given by Eq. (11) with the modified baryon chemical potentials $\mu_b = \varepsilon_b(k = p_b)$.

We also note that the 6-Fermi and 8-Fermi interactions lead to a renormalization of the residual 4-Fermi interactions. The only physical quantities, for which we use the residual 4-Fermi interactions in the $\bar{q}q$ channel to fix model parameters in this work, are the mass of the pion, the pion decay constant, and the $\eta - \eta'$ mass difference, where the pseudoscalar mesons η and η' arise from mixing [100,101] between the η_0 and η_8. The effective 4-Fermi coupling constants in the vacuum, relevant for those quantities, are given by (see, for example, Refs. [101,102] for the 6-Fermi case)

$$\tilde{G}_\pi = \left(G_\pi + \frac{G_8^{(ss)}}{4G_\pi^2}\sigma_{\alpha0}^2\right) - \frac{G_6}{8G_\pi}\sigma_{s0} \equiv 19.04\ \text{GeV}^{-2}, \tag{45}$$

$$\tilde{G}_{00} = \left(G_\pi + \frac{G_8^{(ss)}}{4G_\pi^2}\sigma_{\alpha0}^2\right) + \frac{G_6}{12G_\pi}(2\sigma_0 + \sigma_{s0}), \tag{46}$$

$$\tilde{G}_{08} = -\frac{\sqrt{2}G_6}{12G_\pi}(\sigma_0 - \sigma_{s0}), \tag{47}$$

$$\tilde{G}_{88} = \left(G_\pi + \frac{G_8^{(ss)}}{4G_\pi^2}\sigma_{\alpha0}^2\right) - \frac{G_6}{24G_\pi}(4\sigma_0 - \sigma_{s0}). \tag{48}$$

We require that $\tilde{G}_\pi$ has the same value as G_π in the 4-Fermi calculation in order to reproduce the observed pion mass (see Table I), and that G_6 reproduces the observed mass difference $m_{\eta'} - m_\eta = 0.41$ GeV. One can use Eq. (45) to express the quantity $(G_\pi + \frac{G_8^{(ss)}}{4G_\pi^2}\sigma_{\alpha0}^2)$ in the form $\tilde{G}_\pi + \frac{G_6}{8G_\pi}\sigma_{s0}$. By inserting this into (46) and (48), we see that the three coupling constants (46), (47), and (48), which are used to calculate the $\eta - \eta'$ mass difference, can be expressed in terms of $\tilde{G}_\pi$, G_6, and the quark condensates in the vacuum, $\langle\bar{u}u\rangle_0 = \langle\bar{d}d\rangle_0 = \sigma_0/(4G_\pi)$ and $\langle\bar{s}s\rangle_0 = \sigma_{s0}/(4G_\pi)$, which are fixed by the constituent quark masses in the vacuum and the cutoffs given in Table I. Therefore G_6 can be adjusted to the $\eta - \eta'$ mass difference in the standard way [102], without recourse to the value assumed for $G_8^{(ss)}$. It is also easy to see that the gap equation (40) for the u, d quarks in the vacuum remains numerically the same as in the pure 4-Fermi case because it can be expressed as $M_0 = m - 4\tilde{G}_\pi\langle\bar{u}u\rangle_0$. Therefore, the value of m given in Table I is unchanged.[9] By the standard calculations, we find that $G_6 = 1260\ \text{GeV}^{-5}$ reproduces the observed $\eta - \eta'$ mass difference.

Next we comment on the role of the 8-Fermi coupling constants. As one can expect from the gap equation (40), $G_8^{(ss)}$ works into the same direction as the original 4-Fermi coupling G_π, i.e., it gives attraction, while a positive coupling $G_8^{(sv)}$ gives repulsion. The coupling $G_8^{(vv)}$, on the other hand, is not related to the gap equation, but after eliminating the vector

[9]The value of the current s-quark mass depends slightly on the values assumed for G_6 and $G_8^{(ss)}$. Also the original 4-Fermi coupling constant G_π changes according to Eq. (45), although this has no effect on any physical quantity.

TABLE V. Values of the 6-Fermi coupling constant G_6 in units of GeV^{-5}, and the 8-Fermi coupling constants $G_8^{(ss)}$ and $G_8^{(vv)}$ in units of GeV^{-8}, for the three cases discussed in this section. The coupling $G_8^{(sv)}$ is set to zero in all three cases.

Case	G_6	$G_8^{(ss)}$	$G_8^{(vv)}$
1	0	0	0
2	1260	0	0
3	1260	2330	1220

fields according to (10) it is easily seen to give a repulsive contribution of $4G_8^{(vv)}\rho_\alpha^2\rho_\beta^2 = 81G_8^{(vv)}\rho_B^4$ to the energy density, and $12G_8^{(vv)}\rho_\alpha^2\rho_\beta^2 = 243G_8^{(vv)}\rho_B^4$ to the pressure in symmetric nuclear matter. Although the 8-Fermi coupling constants can be treated as free parameters, their choice is strongly limited by the requirements that the saturation point of isospin-symmetric nuclear matter is unchanged, and the discrepancies of the calculated incompressibility and the symmetry energy to the empirical values do not increase. In the present calculation, we achieved this by making use of the balance between the attractive (ss)-type interaction and the repulsive (vv)-type interaction. Concerning the (sv)-type interaction, which can work as an attraction ($G_8^{(sv)} < 0$) or a repulsion ($G_8^{(sv)} > 0$), we found that the case of attraction leads to conflicts with the nuclear matter equation of state, and the case of repulsion gives a much smaller effect in neutron-star matter than the repulsive (vv)-type interaction. We therefore consider only the case $G_8^{(sv)} = 0$ in the calculations described below. We also note that changes in the original 4-Fermi vector coupling constant G_v, under the constraints imposed by symmetric nuclear matter, do not lead to any noteworthy improvements of the equation of state of neutron-star matter, so we keep the same value as given in Table I.

In Table V, we list as case 1 the pure 4-Fermi case, where the 6-Fermi and 8-Fermi coupling constants are zero, and in case 2 the 6-Fermi interaction with the value of G_6 as determined above is added. Case 3 gives one possible choice for the 8-Fermi coupling constants, where the balance between the attractive (ss)-type interaction and the repulsive (vv)-type interaction is used to keep the nuclear matter properties around the saturation point unchanged, while the (sv)-type interaction is assumed to vanish.

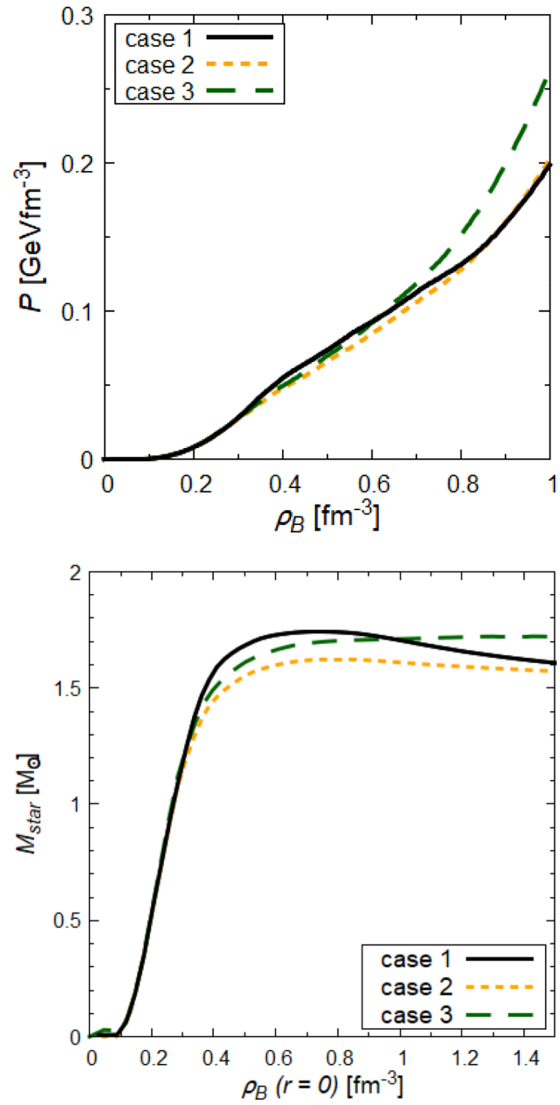

FIG. 9. The pressure in neutron-star matter as function of the baryon density (top panel) and the resulting neutron star masses as function of the central baryon density (bottom panel) for the three cases listed in Table V. Case 1 is identical to the "full result" for the 4-Fermi interaction case, shown by the solid lines in Fig. 8.

B. Numerical results including 6-fermi and 8-fermi interactions

The top panel of Fig. 9 shows the results for the pressure in neutron-star matter for the three cases listed in Table V as functions of the baryon density, and the bottom panel shows the resulting neutron-star masses as functions of the central baryon density. Although the 6-Fermi interaction (case 2) leads only to a slight decrease of the pressure in the region of $\rho_B = 0.35$–0.8 fm^{-3}, the resulting decrease in neutron-star masses is quite significant.[10] On the other hand, the (vv)-type 8-Fermi interaction [last term in Eq. (39)], with a very moderate coupling constant and counterbalanced by the (ss)-type interaction so as not to change the saturation properties of symmetric nuclear matter, gives a strongly increasing pressure for $\rho_B > 0.7$ fm^{-3} and stabilizes the neutron stars against collapse for central densities larger than 0.7 fm^{-3}.

Taken together, the 6-Fermi and 8-Fermi interactions do not lead to noticeable changes of the maximum star masses but rather work towards stabilization of the stars for high central densities. The resulting star masses for case 3 in the range of central densities between 0.7 and 1.5 fm^{-3} are all around $1.7M_\odot$, with radii decreasing from 11.5 km to 9.5 km. We finally give the values of the maximum central baryon densities which gives stable stars, the maximum star masses, and the radii of the stars with maximum mass for the three

[10] As in other works, for example Ref. [26], we find that small changes of the pressure in this region of baryon densities can lead to appreciable changes in the star masses.

cases shown in Fig. 9:

$$\left[\rho_{\rm B}^{\rm max}(r=0),\ M_{\rm star}^{\rm max},\ R\right] = (0.72\ {\rm fm}^{-3},\ 1.73 M_\odot,\ 12.3\ {\rm km})$$

for case 1,

$$\left[\rho_{\rm B}^{\rm max}(r=0),\ M_{\rm star}^{\rm max},\ R\right] = (0.8\ {\rm fm}^{-3},\ 1.62 M_\odot,\ 11.9\ {\rm km})$$

for the case 2, and

$$\left[\rho_{\rm B}^{\rm max}(r=0),\ M_{\rm star}^{\rm max},\ R\right] = (1.4\ {\rm fm}^{-3},\ 1.72 M_\odot,\ 9.8\ {\rm km})$$

for the case 3.

VI. SUMMARY

In this paper we used the three-flavor NJL model as an effective quark theory of QCD to describe the octet baryons as quark-diquark bound states, and the equations of state of nuclear and neutron-star matter in the relativistic mean field approximation based on quark degrees of freedom. One of our basic concepts was to preserve the flavor and chiral symmetries of the interaction Lagrangian, i.e., to allow explicit symmetry breakings only by the current quark masses and not by ad hoc changes of model parameters. In Sec. I we stated the four main purposes of our work, so let us now summarize our results in this order.

First, the internal quark structure of baryons leads to density dependent meson-baryon coupling constants and meson masses which strongly reduce the attractive parts of the interactions in nuclear matter. The main reason for this effect is the nonlinear behavior of the hadron masses as functions of the constituent quark masses. In particular, we found that the attraction experienced by the Σ baryon immersed in nuclear matter is reduced more strongly than that for the Λ baryon, and we could verify that the mass difference between the Σ and Λ baryons immersed in the nuclear medium increases with increasing density. However, we found that this effect, which is based on the different quark-diquark structures of those two baryons, is not sufficient to make the Σ unbound in the region of normal nuclear matter density.

Second, we used concepts of the relativistic Fermi-liquid theory to derive the effective meson exchange interaction between octet baryons in the nuclear medium, and the analog of the Landau relation between the energies of the baryons and the interactions between them. We also used the same concepts to discuss the renormalization of currents carried by baryons, as well as the effects of nucleon density variations on the energies of hyperons immersed in the nuclear medium. To the best of our knowledge, some of these relations cannot be found in the literature, and we hope that our results will be useful for further investigations.

Third, we designed our mean field approximation so that it reflects the basic symmetries of the model and their dynamical breakings, regardless of possible disagreements with observations. To appreciate this point, let us suppose for the moment that we had explicitly broken the flavor and chiral symmetries, as specified below Eq. (1), by choosing a different coupling constant (say G_ρ) for the isovector term in the second line of Eq. (1): $G_\rho[(\bar{q}\lambda_i\gamma^\mu q)^2 + (\bar{q}\lambda_i\gamma^\mu\gamma_5 q)^2]$, where $i = 1, 2, 3$. By choosing $G_\rho \simeq 3G_v \simeq 18\ {\rm GeV}^{-2}$, we could reproduce the empirical symmetry energy $a_s = 32$ MeV (see Sec. III C 3), the shallow bound state of pure neutron matter in Fig. 2 would disappear, neutron stars made of nucleons and leptons would become heavier, and the onset of the Σ^- baryon would move to higher densities or disappear, because its energy gets a positive shift from the vector isovector potential, twice as large as for the neutron [see upper panel of Fig. 7 and Eq. (27)]. This would delay the onset of the decrease of M_s in neutron-star matter (see Fig. 6) and thereby hinder the succession of further hyperons (see lower panel of Fig. 7), leading again to larger star masses. While this ad hoc modification may still have some phenomenological justification, one may think of more drastic changes, such as, for example, enhancing the coupling constant in the vector potential acting on the s quark in Eq. (2), or introducing a phenomenological repulsive function into the energy density which grows asymptotically for large densities. In these or other ways one could "improve" the results, but only little can be learned from it.

Fourth, we found that the so-called hyperon puzzle persists in the NJL model for composite octet baryons in the mean field approximation, and 6-Fermi and 8-Fermi interactions—with coupling constants chosen so as not to spoil the saturation properties of normal nuclear matter—do not solve the problem. On the positive side, we have shown that a special kind of 8-Fermi interaction, characterized by a product of four-quark current operators, is able to support stable stars up to 1.7 solar masses over a large region of central densities. In view of the extremely large baryons densities involved in the investigation of neutron stars, we believe that any solution to the hyperon puzzle must involve quark degrees of freedom, not only quarks in individual hadrons but also quarks which belong to two or more hadrons, or to the whole system. An investigation along these lines would naturally lead to an examination of various patterns of phase transitions to three-flavor quark matter, including pairing and condensation phenomena.

ACKNOWLEDGMENTS

K.N. wishes to thank the staff and students of the Department of Physics at Tokai University for their discussions and advice. W.B. acknowledges very helpful advice from Professor H. Tamura and Professor F. Weber. The work of I.C.C. was supported by the U.S. Department of Energy, Office of Science, Office of Nuclear Physics, contract no. DE-AC02-06CH11357. This work was supported partially through USJHPE (U.S. - Japan Hadronic Physics Exchange Program for Studies of Hadron Structure and QCD) by the U.S. Department of Energy under Grant No. DE-SC0006758.

APPENDIX A: BARYONS AS QUARK-DIQUARK BOUND STATES

The quark-diquark model, based on the static approximation to the Faddeev equation, for octet baryons in the limit of isospin symmetry ($M_u = M_d$) has been described in Refs. [54,67]. As explained in the main text, in our present work we still assume isospin symmetry in the vacuum, and therefore equal current quark masses ($m_u = m_d \equiv m$) and equal constituent quark masses in the vacuum ($M_{u0} = M_{d0} \equiv M_0$). However, a consistent description of isospin-asymmetric

systems, like neutron-star matter, in the framework of an effective quark theory requires to consider the spontaneous breaking of isospin symmetry due to the presence of the medium, i.e., $M_u \neq M_d$. In this Appendix, we therefore briefly explain the main points of our model for the octet baryons, treating the masses M_u, M_d, M_s as independent quantities.

The chiral-invariant interaction Lagrangian in the qq channel is given by [40]

$$\begin{aligned}\mathcal{L}_I^{(qq)} = G_S\big[&\big(\bar{q}\gamma_5 C\lambda_a\lambda_A^{(C)}\bar{q}^T\big)\big(q^T C^{-1}\gamma_5\lambda_a\lambda_A^{(C)}q\big)\\ &-\big(\bar{q}C\lambda_a\lambda_A^{(C)}\bar{q}^T\big)\big(q^T C^{-1}\lambda_a\lambda_A^{(C)}q\big)\big]\\ &+ G_A\big[\big(\bar{q}\gamma_\mu C\lambda_s\lambda_A^{(C)}\bar{q}^T\big)\big(q^T C^{-1}\gamma_\mu\lambda_s\lambda_A^{(C)}q\big)\\ &+\big(\bar{q}\gamma_\mu\gamma_5 C\lambda_a\lambda_A^{(C)}\bar{q}^T\big)\big(q^T C^{-1}\gamma^\mu\gamma_5\lambda_a\lambda_A^{(C)}q\big)\big]. \quad \text{(A1)}\end{aligned}$$

Here λ_a ($a = 2, 5, 7$) are the antisymmetric Gell-Mann flavor matrices, λ_s ($s = 0, 1, 3, 4, 6, 8$) are the symmetric ones, and the antisymmetric Gell-Mann color matrices $\lambda_A^{(C)}$ ($A = 2, 5, 7$) project to color $\bar{3}$ diquark states. (There are also interaction terms in the color 6 diquark channels, which are not shown here because they do not contribute to colorless baryon states.) The charge-conjugation Dirac matrix is $C = i\gamma_2\gamma_0$. The first line in (A1) is the interaction in the scalar diquark (0^+) channel, the second line shows the pseudoscalar diquark (0^-) channel, the third line is the axial vector diquark (1^+) channel, and the fourth line is the vector diquark (1^-) channel. Following previous works [54,67], we include only the scalar and the axial vector diquark channels, which are expected to be dominant from the nonrelativistic analogy.

By simple manipulations in flavor space, we can identically rewrite the two terms relevant for our calculation as follows:

$$\begin{aligned}\mathcal{L}^{(qq)} = G_S&\big(\bar{q}\gamma_5 C t_a\lambda_A^{(C)}\bar{q}^T\big)\big(q^T C^{-1}\gamma_5 t_a^\dagger\lambda_A^{(C)}q\big)\\ &+ G_A\big(\bar{q}\gamma_\mu C t_s\lambda_A^{(C)}\bar{q}^T\big)\big(q^T C^{-1}\gamma_\mu t_s^\dagger\lambda_A^{(C)}q\big), \quad \text{(A2)}\end{aligned}$$

where we introduced the three antisymmetric and anti-Hermitian 3×3 flavor matrices $t_a \equiv (t_{[ud]}, t_{[us]}, t_{[ds]})$, and the six symmetric and Hermitian 3×3 flavor matrices $t_s \equiv (t_{\{ud\}}, t_{\{us\}}, t_{\{ds\}}, t_{\{uu\}}, t_{\{dd\}}, t_{\{ss\}})$. For example, $t_{[ud]}$ is given by

$$t_{[ud]} = \begin{pmatrix} 0 & 1 & 0\\ -1 & 0 & 0\\ 0 & 0 & 0\end{pmatrix}$$

and corresponds to the antisymmetric flavor combination expressed by $[ud]$. The matrices $t_{[us]}$, $t_{[ds]}$ are defined similarly and correspond to the antisymmetric flavor combinations $[us]$ and $[ds]$. The symmetric matrix $t_{\{ud\}}$ has the same structure as $t_{[ud]}$, but with the -1 replaced by $+1$ in the (2,1) component, and corresponds to the symmetric flavor combination expressed by $\{ud\}$. The matrices $t_{\{us\}}$ and $t_{\{ds\}}$ are defined in a similar way for the symmetric flavor combinations $\{us\}$ and $\{ds\}$. Finally, the matrices $t_{\{uu\}}$, $t_{\{dd\}}$, and $t_{\{ss\}}$ have a $\sqrt{2}$ as the (1,1) component, the (2,2) component, and the (3,3) component, respectively, with all other components equal to zero.

We express the Faddeev vertex functions for a given baryon by X_i^a, where a denotes the diquark channels explained above ($a = [ud], \ldots, \{ss\}$), and i is the flavor of the third quark. For example, for the proton the diquark-quark channels are labeled by $[ud]u$, $\{ud\}u$, and $\{uu\}d$. The Faddeev equations for

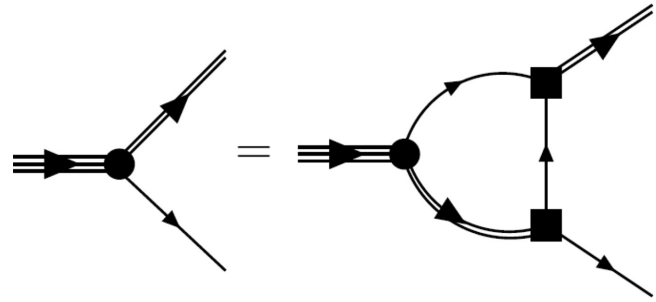

FIG. 10. Graphical representation of the Faddeev equation (A3). The black dot represents the vertex function X, the square the Dirac-flavor vertex functions Λt in (A4), the single lines the quark propagator S, and the double line the diquark propagator τ. External baryon, diquark, and quark lines are amputated.

the vertex functions $X_i^a(p, q)$, describing a baryon of momentum p as a bound state of a quark (momentum q) and a diquark (momentum $p - q$), are

$$X_i^a(p, q) = \int \frac{\mathrm{d}^4k}{(2\pi)^4} Z_{ij}^{ab} S_j(k)\tau_{(ki)}^{bc}(p-k)X_j^c(p, k), \quad \text{(A3)}$$

which is shown graphically in Fig. 10. Here the quark exchange kernel is given by

$$Z_{ij}^{ab} = -3\Lambda^b(t^b S(k+q-p)t^{a\dagger})_{ij}\Lambda^a, \quad \text{(A4)}$$

where the factor -3 comes from projection to color singlet states, and we used the identity $CS^T(k)C^{-1} = S(-k)$ to process the charge-conjugation matrices. The Dirac matrices Λ are given by $\Lambda^a = \gamma_5$ for the scalar diquark channels (flavor index $a = [ud], [us], [ds]$) and $\Lambda^a = \gamma^\mu\gamma_5$ for the axial vector diquark channels (flavor index $a = \{ud\}, \{us\}, \{ds\}, \{uu\}, \{dd\}, \{ss\}$). The quantities $\tau_{(ki)}^{bc}$ in Eq. (A3) are diagonal in the diquark flavor indices, $\tau_{(ki)}^{bc} = \delta_{bc}\tau_{(ki)}^b$, where $\tau_{(ki)}^b$ is the reduced t matrix in the diquark channel b with interacting quark flavors k, i. Therefore, $\tau_{(ki)}^b \equiv \tau_{[ki]}$ in the scalar diquark channels ($[ki] = [ud], [us], [ds]$), and $\tau_{(ki)}^b \equiv \tau_{\{ki\}}^{\mu\nu}$ in the axial vector diquark channels ($\{ki\} = \{ud\}, \{us\}, \{ds\}, \{uu\}, \{dd\}, \{ss\}$). The explicit forms of the reduced diquark t matrices $\tau_{[ki]}$ and $\tau_{\{ki\}}^{\mu\nu}$ are given in Refs. [54,67]. In the last factor $(\ldots)$ of (A4), the quark propagator is considered as a 3×3 diagonal matrix with diagonal elements $S_k = (S_u, S_d, S_s)$.

The formalism described so far is the Faddeev framework in the NJL model, where the only assumptions are the ladder approximation for the two-body t-matrices and the restriction to the scalar and axial vector diquark channels. The quark-diquark model used in the calculations of the main text is obtained by the replacement $S \to -1/M$ in the quark exchange kernel (A4) for each quark flavor k, i.e., this approximation neglects the momentum dependence of the quark exchange kernel and is called the "static approximation" of the Faddeev kernel [76]. In this approximation, the vertex functions X_i^a of (A3) depend only on the total momentum p, and the integral in Eq. (A3) extends only over the product $S_j(k)\tau_{(ki)}^{bc}(p-k)$, which we regularize according to the proper time scheme (see Appendix C), which avoids unphysical thresholds for the decay into quarks. The Dirac structure of

the vertex function can also be determined analytically. Let us again take the proton as an example. Arranging the three interacting channels mentioned above into a vector, the vertex function can be expressed in the form[11]

$$|p\rangle = \begin{pmatrix} X_u^{[ud]}(p) \\ X_u^{\{ud\}}(p) \\ X_d^{\{uu\}}(p) \end{pmatrix} \equiv \begin{pmatrix} \alpha_1[ud]u \\ \left(\alpha_2 \frac{p\!\!\!/}{M_p} + \alpha_3\gamma^\mu\right)\gamma_5\{ud\}u \\ \left(\alpha_4 \frac{p\!\!\!/}{M_p} + \alpha_5\gamma^\mu\right)\gamma_5\{uu\}d \end{pmatrix} u_p(p), \tag{A5}$$

where $u_p(p)$ is the Dirac spinor with the mass of the proton (M_p). Inserting (A5) into Eq. (A3) then gives homogeneous equations for the coefficients α_i, and the characteristic equation gives the proton mass $M_p = M_p(M_u, M_d)$.

The vertex functions of the other members of the octet with two identical quark flavors are similar to (A5), with obvious replacements of quark flavors. For the Σ^0, the flavor structure can be obtained by acting with the isospin-lowering operator (T_-) on $|\Sigma^+\rangle$, which generates

$$|\Sigma^0\rangle = \begin{pmatrix} X_d^{[us]}(p) \\ X_u^{[ds]}(p) \\ X_d^{\{us\}}(p) \\ X_u^{\{ds\}}(p) \\ X_s^{\{ud\}}(p) \end{pmatrix} \equiv \begin{pmatrix} \alpha_1[us]d \\ \alpha_2[ds]u \\ \left(\alpha_3 \frac{p\!\!\!/}{M_{\Sigma^0}} + \alpha_4\gamma^\mu\right)\gamma_5\{us\}d \\ \left(\alpha_5 \frac{p\!\!\!/}{M_{\Sigma^0}} + \alpha_6\gamma^\mu\right)\gamma_5\{ds\}u \\ \left(\alpha_7 \frac{p\!\!\!/}{M_{\Sigma^0}} + \alpha_8\gamma^\mu\right)\gamma_5\{ud\}s \end{pmatrix} u_{\Sigma^0}(p), \tag{A6}$$

where $u_{\Sigma^0}(p)$ is the Dirac spinor with the mass M_{Σ^0}. Note that there is no component with the flavor structure $[ud]s$ in Σ^0, and, of course, also no components where the two light quarks form a scalar diquark in $\Sigma^\pm$ because those vanish identically ($[uu] = [dd] = 0$).

For the Λ, we first construct a state $U_+|\Xi^0\rangle$, where the raising U-spin operator converts an s quark into a d quark, and orthogonalize this state to $|\Sigma^0\rangle$. This gives

$$|\Lambda\rangle = \begin{pmatrix} X_s^{[ud]}(p) \\ X_d^{[us]}(p) \\ X_u^{[ds]}(p) \\ X_d^{\{us\}}(p) \\ X_u^{[ds]}(p) \end{pmatrix} \equiv \begin{pmatrix} \alpha_1[ud]s \\ \alpha_2[us]d \\ \alpha_3[ds]u \\ \left(\alpha_4 \frac{p\!\!\!/}{M_\Lambda} + \alpha_5\gamma^\mu\right)\gamma_5\{us\}d \\ \left(\alpha_6 \frac{p\!\!\!/}{M_\Lambda} + \alpha_7\gamma^\mu\right)\gamma_5\{ds\}u \end{pmatrix} u_\Lambda(p), \tag{A7}$$

where $u_\Lambda(p)$ is the Dirac spinor with the mass M_Λ. Note that there is no component with the flavor structure $\{ud\}s$ in Λ.

In the calculations of the main text we only need the masses of the octet baryons as functions of the constituent quark masses. In isospin-asymmetric systems like neutron-star matter, the isospin symmetry is obviously broken, but the charge symmetry is intact if we simultaneously reverse the signs of the isospin z components of the baryons and the constituent quarks in the baryon. We therefore have the following five independent functions of M_u, M_d (omitting the obvious dependence on M_s for the hyperons to simplify the notations):

$$\begin{aligned} M_p &= M_p(M_u, M_d), \quad M_{\Sigma^+} = M_{\Sigma^+}(M_u), \\ M_{\Xi^+} &= M_{\Xi^+}(M_u), \\ M_{\Sigma^0} &= M_{\Sigma^0}(M_u, M_d) = M_{\Sigma^0}(M_d, M_u), \\ M_\Lambda &= M_\Lambda(M_u, M_d) = M_\Lambda(M_d, M_u). \end{aligned}$$

The masses of the remaining baryons can then be expressed by

$$\begin{aligned} M_n &= M_p(M_d, M_u), \quad M_{\Sigma^-} = M_{\Sigma^+}(M_d), \\ M_{\Xi^0} &= M_{\Xi^+}(M_d). \end{aligned} \tag{A8}$$

The vertex functions and masses of the decuplet baryons are calculated in a similar way. The calculation is simplified by the fact that here only the axial vector diquark channels (symmetric combinations of quark flavors $\{q_1q_2\}$) contribute, which leaves only one possible Dirac-Lorentz structure for all components of the baryon vertex, namely, the Rarita-Schwinger spinor $u^\mu(p, S_b)$.

In the present work, we determined the coupling constants G_S, G_A of the Lagrangian (A1) so as to reproduce the observed masses of the nucleon ($M_N = 0.94$ GeV) and the Delta baryon ($M_\Delta = 1.232$ GeV) in the vacuum ($M_u = M_d = 0.4$ GeV). We also determined our vacuum value of the strange quark mass so as to reproduce the observed mass of the Ω baryon ($M_\Omega = 1.67$ GeV). In this way we obtain

$$G_S = 8.76\ \text{GeV}^{-2}, \quad G_A = 7.36\ \text{GeV}^{-2}, \quad M_s = 0.562\ \text{GeV}. \tag{A9}$$

The resulting masses of octet baryons are given in Table II of the main text. The masses of the decuplet baryons—except for the Δ and the Ω which were fitted—are also well reproduced in this calculation; we obtain $M_{\Sigma^*} = 1.38$ GeV, and $M_{\Xi^*} = 1.53$ GeV. The mass of the kaon, however, is underestimated (0.43 GeV for the case of 4-Fermi couplings); in order to reproduce its observed mass we would need a larger value of M_s. Because the focus of our present work is on the baryons, we made no attempt to reproduce the meson masses well.

The masses of the diquarks [poles of the quantities τ in Eq. (A3)] are $M^{[\ell\ell']} = 0.768$ GeV and $M^{[\ell s]} = 0.902$ GeV for the scalar diquarks with $\ell, \ell' = u, d$, and $M^{\{\ell\ell'\}} = 0.929$ GeV, $M^{\{\ell s\}} = 1.04$ GeV, $M^{\{ss\}} = 1.15$ GeV for the axial vector diquarks.

We finally mention that the values of G_S and G_A given in (A9) are different from those used in a previous work on the flavor SU(2) case [66]. There G_S and G_A were fitted to the mass of the free nucleon and its axial vector coupling constant ($g_A = 1.26$). The values of G_S (G_A) obtained in that way were larger (smaller) than the values given in (A9), which indicates that the dominance of the scalar diquark channel, which increases in-medium because of the decreasing scalar diquark mass, was more pronounced in Ref. [66] than in the present work. This stronger attraction in-medium, however,

[11]The coupling of the time component of the axial vector diquark and the quark to the total spin $(\frac{1}{2}, S_N)$ gives rise to the structure $\frac{p\!\!\!/}{M_N}\gamma_5 u(p, S_N)$, and the coupling of the three-vector components of the axial vector diquark to the quark gives the structure

$$\sum_{\lambda,s}\left(1\tfrac{1}{2}, \lambda s|\tfrac{1}{2}S_N\right)\varepsilon^\mu(p,\lambda)u(p,s) = \frac{-1}{\sqrt{3}}\left(\frac{p^\mu}{M_N} + \gamma^\mu\right)\gamma_5 u(p, S_N),$$

where $\varepsilon^\mu(p,\lambda)$ is the Lorentz four-vector for spin 1 with mass M_N, and $u(p, S_N)$ is the Dirac spinor with mass M_N.

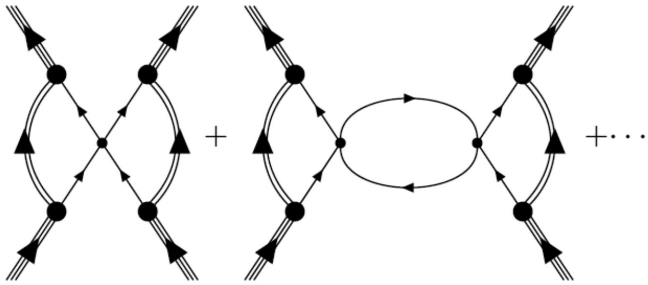

FIG. 11. Graphical representation of a meson exchange interaction in the quark-diquark model for the baryons. Only the quark loop contributions are shown, and the dots indicate the higher orders in the RPA-type series of $\bar{q}q$ bubble graphs. The nucleon loop contributions in the denominators of Eqs. (17) and (18) are not shown here for simplicity. The small dots represent the 4-Fermi interaction in the $\bar{q}q$ channel, and the other symbols are explained in the caption to Fig. 10.

was eventually canceled by a stronger repulsion in the vector-isovector $q\bar{q}$ channel, because in the flavor SU(2) case it was possible to reproduce the symmetry energy in the mean field approximation without violating the chiral symmetry of the interaction Lagrangian. As a result, the pressure in neutron-star matter and the star masses calculated in Ref. [66] were almost identical to the results shown by the dashed lines in Fig. 8 of the main text.

In our present work, we found it more essential to reproduce the $N-\Delta$ mass difference, because one of our motivations was to see how the $\Sigma-\Lambda$ mass difference evolves with density if the spin dependent diquark correlations are constrained to the vacuum value of the $N-\Delta$ mass difference from the outset. The value of g_A, obtained with our present coupling constants (A9), is larger than the observed value by about 10%. In future investigations, we wish to see whether the inclusion of additional diquark channels allows one to find a set of coupling constants which reproduces the nucleon mass, the Delta baryon mass, and g_A simultaneously.

APPENDIX B: MESON EXCHANGE IN SYMMETRIC NUCLEAR MATTER

As mentioned in Sec. III A, in order to express the effective baryon-nucleon interactions (17) and (18) in terms of meson exchange processes of the type shown in Fig. 11, one should multiply the numerator and denominator functions in the first two lines of those expressions by the quark-meson couplings

$$g_\sigma^{(q)2} = g_\delta^{(q)2} = \frac{-1}{\Pi_s'(q^2=0)}, \tag{B1}$$

and similarly in the third lines by

$$g_\omega^{(q)2} = g_\rho^{(q)2} = \frac{-1}{\Pi_v'(q^2=0)}. \tag{B2}$$

Here the $\bar{q}q$ bubble graphs in the scalar and vector channels are given by

$$\Pi_s(q^2) = 12i\int\frac{\mathrm{d}^4k}{(2\pi)^4} \times\left[\frac{-2}{k^2-M^2}+(q^2-4M^2) \times\int_0^1\mathrm{d}x\frac{1}{[k^2-M^2+q^2x(1-x)]^2}\right], \tag{B3}$$

$$\Pi_v(q^2) = 48iq^2\int\frac{\mathrm{d}^4k}{(2\pi)^4}\int_0^1\mathrm{d}x\frac{x(1-x)}{[k^2-M^2+q^2x(1-x)]^2}, \tag{B4}$$

and the primes in (B1) and (B2) mean differentiation with respect to q^2.

For simplicity we consider only the $\ell=0$ terms in (17) and (18). They can be expressed in the following form:

$$f_{0,bN} = -\frac{M_b}{E_b}\frac{M_N}{E_N}\frac{g_\sigma^{(b)}g_\sigma^{(N)}}{M_\sigma^2}+\frac{g_\omega^{(b)}g_\omega^{(N)}}{M_\omega^2}, \tag{B5}$$

$$f'_{0,bN} = -\frac{M_b}{E_b}\frac{M_N}{E_N}\frac{g_\delta^{(b)}g_\delta^{(p)}}{M_\delta^2}+\frac{g_\rho^{(b)}g_\rho^{(p)}}{M_\rho^2}. \tag{B6}$$

Here all meson-baryon coupling constants and meson masses are defined at zero momentum, and are different from the values at the meson poles. The resulting values for the effective coupling constants and masses are summarized for three values of the baryon density in Table VI. In relation to our discussions in Sec. III C, we note that $g_\sigma^{(\Lambda)} > g_\sigma^{(\Sigma)}$, which reflects the different internal quark-diquark structure of the Λ and the Σ baryons.

We finally add a few comments on the definition of effective coupling constants and meson masses used here: First, the multiplication of the density dependent scaling factors (B1) and (B2) to the numerators and denominators of (17) and (18) obscures the simplicity of those basic expressions, and for better orientation the values listed in Table IV of the main text is more useful. Nevertheless, it is necessary for a proper definition of coupling constants and meson masses at zero momentum of the mesons. For the coupling constants, this is immediately clear from Fig. 11. For the meson masses, consider for example the case of the σ meson. The reduced t matrix in the 0^+ $\bar{q}q$ channel is given by

$$\tau_\sigma(q^2) = \frac{-2G_\pi}{1+2G_\pi\Pi_s(q^2)+2G_\pi\delta M_\sigma^2}, \tag{B7}$$

where the nucleon loop contributions, approximated by their forms at $q=0$, are denoted by δM_σ^2. Expanding (B7) around $q^2=0$ gives the approximate Yukawa-like form

$$\tau_\sigma(q^2) = \frac{g_\sigma^{(q)2}}{q^2-M_\sigma^2},$$

where $g_\sigma^{(q)}$ is defined by (B1), and

$$M_\sigma^2 = g_\sigma^{(q)2}\left(\frac{1}{2G_\pi}+\Pi_s(q^2=0)+\delta M_\sigma^2\right). \tag{B8}$$

TABLE VI. Effective coupling constants and masses of σ, ω, δ, and ρ mesons for four values of the baryon density in symmetric nuclear matter. Coupling constants are dimensionless, and masses are given in units of GeV. For definitions, see Eqs. (B5), (B6), and the text.

Density	$g_\sigma^{(q)}$	$g_\sigma^{(N)}$	$g_\sigma^{(\Lambda)}$	$g_\sigma^{(\Sigma)}$	$g_\sigma^{(\Xi)}$	M_σ
0	6.63	18.21	12.13	10.28	5.70	1.25
0.15	4.85	10.06	7.05	5.59	3.15	0.96
0.3	4.20	6.25	4.80	3.59	2.06	0.97
0.5	3.85	4.01	3.45	2.44	1.43	1.05
Density	$g_\omega^{(q)}$	$g_\omega^{(N)}$	$g_\omega^{(\Lambda)}$	$g_\omega^{(\Sigma)}$	$g_\omega^{(\Xi)}$	M_ω
0	5.27	15.80	10.54	10.54	5.27	1.52
0.15	4.51	13.53	9.02	9.02	4.51	1.30
0.3	4.18	12.53	8.35	8.35	4.18	1.20
0.5	3.99	11.96	7.97	7.97	3.99	1.15
Density	$g_\delta^{(q)}$	$g_\delta^{(p)}$	$g_\delta^{(\Lambda)}$	$g_\delta^{(\Sigma^+)}$	$g_\delta^{(\Xi^0)}$	M_δ
0	6.63	4.64	0	10.28	5.70	1.25
0.15	4.85	2.38	0	5.59	3.15	0.99
0.3	4.20	1.38	0	3.59	2.06	1.00
0.5	3.85	0.81	0	2.44	1.43	1.10
Density	$g_\rho^{(q)}$	$g_\rho^{(p)}$	$g_\rho^{(\Lambda)}$	$g_\rho^{(\Sigma^+)}$	$g_\rho^{(\Xi^0)}$	M_ρ
0	5.27	5.27	0	10.54	5.27	1.52
0.15	4.51	4.51	0	9.02	4.51	1.30
0.3	4.18	4.18	0	8.35	4.18	1.20
0.5	3.99	3.99	0	7.97	3.99	1.15

The terms $(\dots)$ in (B8) agree with the denominator in the second line of Eq. (17) because of the relation $\Pi_s(q^2=0) = 2g(M)$, where $g(M)$ is given by Eq. (19).

APPENDIX C: REGULARIZATION METHOD

To evaluate four-dimensional integrals, we introduce Feynman parameters and perform shifts of the loop momentum so that the integrand depends only on k^2, where k is the loop momentum, besides other fixed variables. We then perform a Wick rotation and use four-dimensional spherical polar coordinates to obtain

$$\int \mathrm{d}^4k f(k^2) = 2\pi^2 i \int_0^\infty \mathrm{d}k_E k_E^3 f\left(-k_E^2\right),$$

where $k_E = (k_0^2 + \boldsymbol{k}^2)^{1/2}$ is the Euclidean length. Next, we consider the following identities:

$$\ln\frac{D}{D_0} = -\int_0^\infty \frac{\mathrm{d}\tau}{\tau}(e^{-\tau D} - e^{-\tau D_0}), \tag{C1}$$

$$\frac{1}{D^n} = \frac{1}{(n-1)!}\int_0^\infty \mathrm{d}\tau \tau^{n-1} e^{-\tau D}\ (n \geqslant 0), \tag{C2}$$

where D is a function of k_E^2 and other fixed variables. In the proper time regularization scheme, the infrared cutoff (Λ_{IR}) is introduced by replacing the upper integration limits in (C1) and (C2) by $1/\Lambda_{\mathrm{IR}}^2$, and the ultraviolet cutoff (Λ_{UV}) by replacing the lower integration limits by $1/\Lambda_{\mathrm{UV}}^2$. After these replacements, one performs the integration over k_E. The ultraviolet cutoff makes the integrals finite, while the infrared cutoff eliminates unphysical thresholds (imaginary parts) for the decay of hadrons into quarks, thus simulating the role of confinement.

APPENDIX D: SIZES OF QUARK CORES IN THE NUCLEAR MEDIUM

The rms radius of the baryon density distribution of the quark core of the nucleons in the medium is related to the isoscalar combination of the corresponding electric charge radii of protons and neutrons by

$$r_N(\rho_B) = \sqrt{\langle r_{Ep}^2\rangle(\rho_B) + \langle r_{En}^2\rangle(\rho_B)}. \tag{D1}$$

In the language of Feynman diagrams used in Ref. [103], the corresponding isoscalar baryon form factor is obtained by the operator insertion $\frac{1}{3}\gamma^0$ on each quark line. For free nucleons (zero density) the result of the NJL model calculations of Ref. [103], using the same parameters as in the present paper, is $r_N(0) = 0.475$ fm. Note that this is the value for the quark core without meson cloud corrections, obtained by replacing the dressed quark form factors in Sec. VI of Ref. [103] by their bare values ($F_{1U} = \frac{2}{3}, F_{1D} = -\frac{1}{3}, F_{2U} = F_{2D} = 0$). The pion cloud contributions to the isoscalar quantity r_N are very small. A simple estimate of ω meson cloud effects, using our present value of G_v, gives only a small correction, but a more realistic treatment, following the lines of the vector meson dominance model with the observed ω meson pole, increases the isoscalar baryon radius to 0.78 fm (see Table VI of Ref. [103]), which is close to the experimental value. As mentioned in the main text, however, the quantity which seems more relevant for the role of the Pauli principle is the baryon radius of the quark core without meson cloud effects. This is simply because the mesons are bosons, and the overlap of the meson clouds just corresponds to the meson exchange interactions. Therefore the results shown in Sec. III C 5 of the main text refer to this quantity.

Based on naive geometric intuition, the volume fraction occupied by the quark cores can be defined as

$$f(\rho_B) = \rho_B v_N(\rho_B), \tag{D2}$$

where $v_N(\rho_B) = \frac{4\pi}{3} r_N^3(\rho_B)$. Estimates based on this expression are also given in the main text.

[1] J. Haidenbauer and Ulf-G. Meißner, Phys. Rev. C **72**, 044005 (2005).
[2] T. A. Rijken and Y. Yamamoto, Phys. Rev. C **73**, 044008 (2006).
[3] S. K. Bogner, R. J. Furnstahl, and A. Schwenk, Prog. Part. Nucl. Phys. **65**, 94 (2010).
[4] S. Petschauer, J. Haidenbauer, N. Kaiser, U.-G. Meißner, and W. Weise, Front. Phys. **8**, 12 (2020).

[5] D. Lonardoni, F. Pederiva, and S. Gandolfi, Phys. Rev. C **89**, 014314 (2014).
[6] A. Faessler, F. Fernandez, G. Lubeck, and K. Shimizu, Phys. Lett. B **112**, 201 (1982).
[7] M. Oka, K. Shimizu, and K. Yazaki, Nucl. Phys. A **464**, 700 (1987).
[8] Y. Fujiwara, Y. Suzuki, and C. Nakamoto, Prog. Part. Nucl. Phys. **58**, 439 (2007).
[9] M. Oka, arXiv:2301.06026.
[10] T. Inoue, N. Ishii, S. Aoki, T. Doi, T. Hatsuda, Y. Ikeda, K. Murano, H. Nemura, and K. Sasaki (HAL QCD Collaboration), Prog. Theor. Phys. **124**, 591 (2010).
[11] T. Hyodo and M. Niiyama, Prog. Part. Nucl. Phys. **120**, 103868 (2021).
[12] T. Motoba and S. Sugimoto, in *Proceedings of the 10th International Conference on Hypernuclear and Strange Particle Physics (HYP 2009), Tokai, Japan*, edited by B. F. Gibson, K. Imai, T. Motoba, T. Nagae, and A. Ohnishi (2009); Nucl. Phys. A **835**, 223 (2010).
[13] A. Gal, E. V. Hungerford, and D. J. Millener, Rev. Mod. Phys. **88**, 035004 (2016).
[14] E. Hiyama and K. Nakazawa, Annu. Rev. Nucl. Part. Sci. **68**, 131 (2018).
[15] H. Tamura, EPJ Web Conf. **271**, 12001 (2022).
[16] K. Miwa *et al.*, EPJ Web Conf. **271**, 04001 (2022).
[17] T. Nanamura *et al.* (J-PARC E40 Collaboration), PTEP **2022**, 093D01 (2022).
[18] P. Demorest, T. Pennucci, S. Ransom, M. Roberts, and J. Hessels, Nature (London) **467**, 1081 (2010).
[19] J. Antoniadis *et al.*, Science **340**, 1233232 (2013).
[20] T. E. Riley *et al.*, Astrophys. J. Lett. **918**, L27 (2021).
[21] E. Fonseca *et al.*, Astrophys. J. Lett. **915**, L12 (2021).
[22] N. K. Glendenning, *Compact Stars: Nuclear Physics, Particle Physics, and General Relativity* (Springer, New York, 1997).
[23] I. Bombaci, JPS Conf. Proc. **17**, 101002 (2017).
[24] D. Chatterjee and I. Vidaña, Eur. Phys. J. A **52**, 29 (2016).
[25] G. F. Burgio, H. J. Schulze, I. Vidana, and J. B. Wei, Prog. Part. Nucl. Phys. **120**, 103879 (2021).
[26] S. Weissenborn, D. Chatterjee, and J. Schaffner-Bielich, Phys. Rev. C **85**, 065802 (2012); Erratum: **90**, 019904 (2014).
[27] W. M. Spinella and F. Weber, Astron. Nachr. **340**, 145 (2019).
[28] Y. Yamamoto, T. Furumoto, N. Yasutake, and T. A. Rijken, Phys. Rev. C **88**, 022801(R) (2013).
[29] J. Haidenbauer, U. G. Meißner, N. Kaiser, and W. Weise, Eur. Phys. J. A **53**, 121 (2017).
[30] M. Kohno, Phys. Rev. C **97**, 035206 (2018).
[31] D. Logoteta, I. Vidana, and I. Bombaci, Eur. Phys. J. A **55**, 207 (2019).
[32] D. Gerstung, N. Kaiser, and W. Weise, Eur. Phys. J. A **56**, 175 (2020).
[33] G. A. Contrera, D. Blaschke, J. P. Carlomagno, A. G. Grunfeld, and S. Liebing, Phys. Rev. C **105**, 045808 (2022).
[34] M. Buballa, Phys. Rep. **407**, 205 (2005).
[35] M. G. Alford, A. Schmitt, K. Rajagopal, and T. Schäfer, Rev. Mod. Phys. **80**, 1455 (2008).
[36] P. A. M. Guichon, Phys. Lett. B **200**, 235 (1988).
[37] A. Chodos, R. L. Jaffe, K. Johnson, C. B. Thorn, and V. F. Weisskopf, Phys. Rev. D: Part. Fields **9**, 3471 (1974).
[38] Y. Nambu and G. Jona-Lasinio, Phys. Rev. **122**, 345 (1961).
[39] Y. Nambu and G. Jona-Lasinio, Phys. Rev. **124**, 246 (1961).
[40] U. Vogl and W. Weise, Prog. Part. Nucl. Phys. **27**, 195 (1991).
[41] T. Hatsuda and T. Kunihiro, Phys. Rep. **247**, 221 (1994).
[42] N. Ishii, W. Bentz, and K. Yazaki, Nucl. Phys. A **587**, 617 (1995).
[43] W. Bentz and A. W. Thomas, Nucl. Phys. A **696**, 138 (2001).
[44] D. F. Geesaman, K. Saito, and A. W. Thomas, Annu. Rev. Nucl. Part. Sci. **45**, 337 (1995).
[45] D.-H. Lu, A. W. Thomas, K. Tsushima, A. G. Williams, and K. Saito, Phys. Lett. B **417**, 217 (1998).
[46] J. R. Stone, P. A. M. Guichon, P. G. Reinhard, and A. W. Thomas, Phys. Rev. Lett. **116**, 092501 (2016).
[47] I. C. Cloët, W. Bentz, and A. W. Thomas, Phys. Rev. Lett. **95**, 052302 (2005).
[48] I. C. Cloët, W. Bentz, and A. W. Thomas, Phys. Lett. B **642**, 210 (2006).
[49] I. C. Cloët, W. Bentz, and A. W. Thomas, Phys. Rev. Lett. **116**, 032701 (2016).
[50] K. Saito, K. Tsushima, and A. W. Thomas, Prog. Part. Nucl. Phys. **58**, 1 (2007).
[51] F. Sammarruca, arXiv:0801.0879.
[52] P. A. M. Guichon, A. W. Thomas, and K. Tsushima, Nucl. Phys. A **814**, 66 (2008).
[53] F. E. Close, *An Introduction to Quarks and Partons* (Academic Press, 1979).
[54] M. E. Carrillo-Serrano, W. Bentz, I. C. Cloët, and A. W. Thomas, Phys. Lett. B **759**, 178 (2016).
[55] L. D. Landau, Sov. Phys. JETP **3**, 920 (1956).
[56] L. D. Landau, Sov. Phys. JETP **5**, 101 (1957).
[57] L. D. Landau, Sov. Phys. JETP **8**, 70 (1959).
[58] A. B. Migdal, *Theory of Finite Fermi Systems and Applications to Atomic Nuclei* (Wiley, New York, 1967).
[59] A. B. Migdal, E. E. Saperstein, M. A. Troitsky, and D. N. Voskresensky, Phys. Rep. **192**, 179 (1990).
[60] G. Baym and S. A. Chin, Nucl. Phys. A **262**, 527 (1976).
[61] P. Nozières, *Theory of Interacting Fermi Systems* (W. A. Benjamin, New York, 1964).
[62] J. Negele and H. Orland, *Quantum Many-Particle Systems* (Westview Press, 1998).
[63] R. Shankar, Rev. Mod. Phys. **66**, 129 (1994).
[64] G. 't Hooft, Phys. Rev. D **14**, 3432 (1976); Erratum: **18**, 2199 (1978).
[65] A. A. Osipov, B. Hiller, A. H. Blin, and J. da Providência, Ann. Phys. (NY) **322**, 2021 (2007).
[66] T. Tanimoto, W. Bentz, and I. C. Cloët, Phys. Rev. C **101**, 055204 (2020).
[67] M. E. Carrillo-Serrano, I. C. Cloët, and A. W. Thomas, Phys. Rev. C **90**, 064316 (2014).
[68] K. Saito and A. W. Thomas, Phys. Lett. B **327**, 9 (1994).
[69] M. C. Birse, Phys. Rev. C **51**, R1083 (1995).
[70] K. Saito and A. W. Thomas, Phys. Rev. C **52**, 2789 (1995).
[71] S. J. Wallace, F. Gross, and J. A. Tjon, Phys. Rev. Lett. **74**, 228 (1995).
[72] G. E. Brown and W. Weise, Comments Nucl. Part. Phys. **17**, 39 (1987).
[73] S. J. Wallace, Nucl. Phys. A **631**, 137 (1998).
[74] W. Bentz, A. Arima, H. Hyuga, K. Shimizu, and K. Yazaki, Nucl. Phys. A **436**, 593 (1985).
[75] J. S. Schwinger, Phys. Rev. **82**, 664 (1951).
[76] G. Hellstern, R. Alkofer, and H. Reinhardt, Nucl. Phys. A **625**, 697 (1997).
[77] M. Gell-Mann, Phys. Rev. **125**, 1067 (1962).

[78] S. Okubo, Prog. Theor. Phys. **27**, 949 (1962).
[79] W. Bentz, T. Horikawa, N. Ishii, and A. W. Thomas, Nucl. Phys. A **720**, 95 (2003).
[80] K. Nagata and A. Hosaka, Prog. Theor. Phys. **111**, 857 (2004).
[81] S. Ulrych and H. Muther, Phys. Rev. C **56**, 1788 (1997).
[82] W. Bentz and I. C. Cloët, Phys. Rev. C **105**, 014320 (2022).
[83] J. A. McNeil, R. D. Amado, C. J. Horowitz, M. Oka, J. R. Shepard, and D. A. Sparrow, Phys. Rev. C **34**, 746 (1986).
[84] S. Ichii, W. Bentz, A. Arima, and T. Suzuki, Nucl. Phys. A **487**, 493 (1988).
[85] J. Cohen and R. J. Furnstahl, Phys. Rev. C **35**, 2231 (1987).
[86] J. Cohen, Phys. Rev. C **48**, 1346 (1993).
[87] A. Arima, K. Shimizu, W. Bentz, and H. Hyuga, Adv. Nucl. Phys. **18**, 1 (1987).
[88] R. J. Furnstahl and B. D. Serot, Nucl. Phys. A **468**, 539 (1987).
[89] P. K. Panda, M. E. Bracco, M. Chiapparini, E. Conte, and G. Krein, Phys. Rev. C **65**, 065206 (2002).
[90] J. Leong, A. W. Thomas, and P. A. M. Guichon, arXiv:2308.08987.
[91] S. Okubo, Phys. Lett. **5**, 165 (1963).
[92] G. Zweig, An SU(3) model for strong interaction symmetry and its breaking. Version 2, in *Developments in the Quark Theory of Hadrons, 1964–1978*, edited by D. B. Lichtenberg and S. P. Rosen (Hadronic Press, 1980), Vol. 1, pp. 22–101.
[93] J. Iizuka, Prog. Theor. Phys. Suppl. **37**, 21 (1966).
[94] H. Heiselberg and M. Hjorth-Jensen, Phys. Rep. **328**, 237 (2000).
[95] J. R. Stone, V. Dexheimer, P. A. M. Guichon, A. W. Thomas, and S. Typel, Mon. Not. R. Astron. Soc. **502**, 3476 (2021).
[96] T. F. Motta and A. W. Thomas, Mod. Phys. Lett. A **37**, 2230001 (2022).
[97] J. Leong, T. F. Motta, A. W. Thomas, and P. A. M. Guichon, Phys. Rev. C **108**, 015804 (2023).
[98] R. C. Tolman, Phys. Rev. **55**, 364 (1939).
[99] J. R. Oppenheimer and G. M. Volkoff, Phys. Rev. **55**, 374 (1939).
[100] T. Hatsuda and T. Kunihiro, Z. Phys. C: Part. Fields **51**, 49 (1991).
[101] P. Rehberg, S. P. Klevansky, and J. Hufner, Phys. Rev. C **53**, 410 (1996).
[102] M. Katô, W. Bentz, K. Yazaki, and K. Tanaka, Nucl. Phys. A **551**, 541 (1993).
[103] I. C. Cloët, W. Bentz, and A. W. Thomas, Phys. Rev. C **90**, 045202 (2014).